CHALMERS
UNIVERSITY OF TECHNOLOGY

Evaluation of the flexibility of large and complex heat exchanger networks

A case study at Södra Cell Mönsterås

Master's thesis in Sustainable Energy Systems

PONTUS BOKINGE
DAVID ERLANDSSON

Department of Space, Earth and Environment
Division of Energy Technology
CHALMERS UNIVERSITY OF TECHNOLOGY
Gothenburg, Sweden 2018

Master's thesis 2018

Evaluation of the flexibility of large and complex heat exchanger networks

A case study at Södra Cell Mönsterås

PONTUS BOKINGE
DAVID ERLANDSSON

CHALMERS
UNIVERSITY OF TECHNOLOGY

Department of Space, Earth and Environment
Division of Energy Technology
Chalmers University of Technology
Gothenburg, Sweden 2018

Evaluation of the flexibility of large and complex heat exchanger networks
A case study at Södra Cell Mönsterås
PONTUS BOKINGE
DAVID ERLANDSSON

Supervisors: Christian Langner, Department of Space, Earth and Environment
Elin Svensson, CIT Industriell Energi

Examiner: Simon Harvey, Department of Space, Earth and Environment

Master's Thesis 2018
Department of Space, Earth and Environment
Division of Energy Technology
Chalmers University of Technology
SE-412 96 Gothenburg
Telephone +46 31 772 1000

Cover: A photo showing an overview of Södra Cell Mönsterås (Courtesy of Södra).

Typeset in LaTeX
Printed by Chalmers Reproservice
Gothenburg, Sweden 2018

Evaluation of the flexibility of large and complex heat exchanger networks
A case study at Södra Cell Mönsterås

PONTUS BOKINGE & DAVID ERLANDSSON
Department of Space, Earth and Environment
Chalmers University of Technology

Abstract

The Swedish Energy Agency is commissioned by the national government to ensure that Swedish energy use is 50 % more efficient by 2030 compared to 2005. The pulp and paper industry represents almost 20 % of final energy consumption in Sweden and improvements in this sector are essential to achieve the overall efficiency targets.

Heat exchanger networks, used to recover energy in for example the pulp and paper industry, are often designed for one set of operating conditions. However, industrial processes must be flexible and able to adapt to e.g. seasonal variations and changes in feedstock or production volume. Thus, the design of heat exchanger networks should account for several sets of operating conditions, in order to ensure consistently low energy use without negative impact on the overall process.

Analysing several prospected designs at a range of operating conditions requires a large number of calculations, and simulation models may be necessary. However, setting up simulation models is time consuming and a more straightforward way to screen design proposals in the early design phase is called for. In this work, a MATLAB-tool is developed which allows fast evaluation of the heat exchanger network response for any given structure when operating conditions and/or operational settings are manipulated. A case study on the heat exchanger networks of a large Kraft Pulp Mill is performed, where different retrofit designs are analysed for spring, winter and summer conditions using the developed tool. Operational settings are manipulated in order to maximise steam savings for each season, allowing a fair comparison between the designs.

The best design obtains 6.6 MW of steam savings during spring operation. This is 23.8 % of the theoretical energy savings identified by a pinch analysis of the process. All designs fulfil the flexibility requirements imposed by the seasonal variations. The best design achieves this with steam savings which are 6.7-17.3 % higher than the worst design, depending on season, while using less new equipment. Additionally, steam savings for the investigated designs are shown to increase by up to 22.4 % when operational settings are adjusted to suit new operating conditions, compared to using operational settings optimised for other conditions.

Keywords: Flexibility, Heat exchanger network, Retrofit, Pinch Analysis, Södra Cell, Kraft Pulp Mill, Seasonal variations

Acknowledgements

A special thanks goes to our main supervisor Christian Langner who did an excellent job. Always showing engagement and providing constructive feedback during the whole time of the work. Also a great thanks to our supervisor Elin Svensson at CIT. Providing us with expert insights within the area of pinch analysis and continuously constructive feedback on both the project and report.

Thanks to Södra for their hospitality during our visit. Specially thanks to Karin Dernegård and Örjan Johansson who have provided good discussions during the work of this thesis and for their expertise of the mill.

Finally, a great thanks to the Division of Energy Technology for the warm hospitality during all days of the week.

Pontus Bokinge & David Erlandsson, Gothenburg, June 2018

Contents

List of Figures

List of Tables

Abbreviations

HEN-S - The name of the developed MATLAB-tool. (Heat Exchanger Network Solver)

SHS - Secondary heating system

HEN - Heat exchanger network

HEX - Heat exchanger

N&M - Refers to the Master's Thesis work done by Nihlmark and Mahmoud [7]

GCC - Grand composite curve

CW - Cold water (15 °C)

WW - Warm water (55 °C)

HW - Hot water (85 °C)

VHW - Very hot water (100+ °C)

MER - Maximum energy recovery

$Q_{H,min}$ - Theoretical minimum heating demand

$Q_{H,actual}$ - Actual heating demand

ΔT_{min} - Minimum temperature difference between a process-to-process heat exchanger when performing a pinch analysis.

1
Introduction

The task of reducing society's energy use has reached the highest political level, and both the EU and the Swedish government have established targets for improved energy efficiency. The EU Energy Efficiency Directive of 2012 requires member states to increase energy efficiency by 30 % by 2030 compared to 2007 [1]. In Sweden, the Energy Agency is commissioned by the government to ensure that the Swedish energy use is 50 % more efficient[1] by 2030 compared to 2005[2]. Consequently, Swedish industries must reduce their energy use substantially in the upcoming decade. Industrial energy use in Sweden is dominated by the pulp and paper industry, with 52 % of the total industrial energy use [3]. Therefore, improvements in pulp and paper industry are essential to achieve the overall energy efficiency targets.

The largest pulp mill in southern Sweden is Södra Cell Mönsterås which has more than 400 employees and produces 750 000 tonnes of pulp annually. Apart from pulp, the plant also exports heat and power to surrounding companies and the municipality. In order to respond to the targets established by the Swedish Energy Agency and the EU Energy Efficiency Directive, Södra has initialised research and energy efficiency projects. The goal is to reduce heat and electricity use by 10 % by 2025 compared to 2015. Since the plant operates throughout the year, seasonal variations and market conditions affect the process. In order to respond to changing conditions and act efficiently all year around flexibility of the process is important and must be considered during energy efficiency projects. [4, 5]

1.1 Background

A new research project in collaboration between Chalmers, Södra and the Swedish Energy Agency aims to establish guidelines for the design of heat exchanger networks with high flexibility and operability [6]. This will make energy efficiency and flexibility compatible in process design, thus increasing both the energy savings potential and the practical feasibility of energy efficiency projects.

In 2017, Nihlmark and Mahmoud [7] mapped the energy systems at Södra Cell Mönsterås with special focus on the plant's secondary heating system. In particular, properties such as flowrate and start and target temperatures were identified for major process streams. Additionally, actual and minimum utility consumption for the process were established. The data was extracted during springtime operation

[1] Measured as supplied energy per GDP

with high production rate of softwood pulp, and is thus suitable for investigating energy efficiency projects at the plant during these conditions. [7]

In industrial processes, energy efficiency is often obtained by increased heat integration. Theoretical energy targets through heat integration can be calculated using a method called pinch analysis, which also provide guidelines for designing heat exchanger networks that can achieve those savings. A thorough introduction to pinch analysis is given in [8] and a brief summary is given in Section 2.1 of this report. The energy savings that can be achieved using pinch analysis are often large in theory, but limited by practical and economic considerations. For example, high energy efficiency often requires a large number of heat exchanger units, and is associated with high capital costs. Furthermore, industrial processes must be flexible. This means that product quality must be maintained during a range of different operating conditions and process disturbances. Thus, the heat exchanger network must be designed to ensure that all involved process streams reach their predefined target temperatures under changing conditions.

The flexibility of a heat exchanger network is defined as its ability to reach target process stream temperatures during varying operating conditions [9, 10, 11, 12]. Cerda et al. [13] took the concept further and defined a heat exchanger network to be structurally flexible if it combines flexibility with maximum energy recovery. Below, the term structural flexibility is used with a slightly different meaning. In this work, the flexibility of a network, as defined above, is seen as the combination of *structural* flexibility and *energy* flexibility. Structural flexibility of a network is the possibility to adjust operational settings, such as split ratios and bypass ratios of heat exchangers, to reach target temperatures. Note the distinction made above between operating conditions, set externally by for example ambient conditions and production mix, and operational settings, which can be adjusted during operation. If targets cannot be reached through structural flexibility alone, energy flexibility is required. This flexibility is the possibility to reach target temperatures by using external utility. If a certain level of flexibility is required in a HEN, i.e. if a set of target temperatures must be reached for specified sets of operating conditions, the combined structural and energy flexibility must be high enough to reach it. The higher the structural flexibility of the network, the lower the need for external utility and hence for energy flexibility. The amount of external utility required for a level of flexibility can thus be seen as an indirect measure of the structural flexibility in the network.

When heat exchanger networks are developed to recover energy, processes become more interconnected. If flexibility is not addressed during the design of such networks, overall process flexibility is likely to deteriorate. This may discourage investments in energy efficiency projects. Conversely, if flexibility is explicitly considered in the design phase, experience shows that process flexibility may actually improve as a result of increased heat integration [8, 14]. It should be stressed that while flexibility is important with respect to maintaining product quality, high structural flexibility is important to ensure low energy use during changing conditions. A heat

exchanger network that is optimised for high energy efficiency at one set of operating conditions, is often far from optimal at other conditions, unless the network is able to adapt to changes [8, 14, 15, 16]. Thus, the design of heat exchanger networks should consider more than just one set of operating conditions.

Operating conditions in a process may change both intentionally, due to variations in production mix and volume over a year, and due to actual factors such as equipment fouling and seasonal variations [8, 14]. In this work variations of operating conditions are limited to include the effect of seasonal variations. Short term variations, such as process disturbances and change of production mix, are filtered to be consistent with the data extraction of Nihlmark & Mahmoud and the criteria are described in Section 5.5. A data set is extracted for every season of the year with filtering making sure that no short term variations and variation in production mix occur.

To account for seasonal variations during heat exchanger network design, the performance of a proposed design must be evaluated at different operating conditions. However, simply providing a network model with new input data to reflect the new operating conditions, and evaluating the resulting effect on target temperatures and utility consumption, does not give a realistic view of actual network performance at the new operating conditions. If operational settings in the network can be adjusted between operating conditions (i.e., if the network has structural flexibility), this should be accounted for during performance evaluation. Consequently, a thorough investigation of network performance during changing conditions should include not only changes in operating conditions, but also a tuning of operational settings to suit the new conditions. Different operating conditions may also motivate design changes, in terms of over-designing heat exchangers for the initial operating conditions to better suit one of the other investigated conditions. Thus, structural flexibility can be achieved by over-sizing heat transfer areas, but how much is optimal from a cost perspective? In order to optimise the network a trade-off between energy, structural flexibility and capital need to be considered.

Investigating a range of operational settings, considering potentially increased heat exchanger sizes and tuning of operational settings, quickly becomes a tedious task to perform by hand. A simulation model can be set up to perform the required calculations. However, this is in itself time consuming and in an early design phase, several design options in terms of network structure may exist. This means individual simulation models must be set up for each prospective design.

The discussion above illustrates the need for a general computational tool or method which can be easily applied to any network design, thus avoiding the time consuming task of setting up multiple simulation models, and be used to evaluate the effect of changing operating conditions and settings.

The use of “Sensitivity table”, first introduced by B. Linnhoff and E. Kotjabasakis [14], is a step towards such a method. These tables are derived by using simplified

mathematical models of heat exchanger networks to estimate the effect that changes in supply temperatures, heat capacity flowrates and UA-values will have on target temperatures. The characteristics of the simplified models mean that the sensitivity tables can be generated in an automatic way for any given heat exchanger network. This gives a way of estimating the impact of changes in operating conditions (supply temperatures and flowrates) that is much faster than complete simulations. Additionally, the effect of changing operational settings (bypassing heat exchangers) or re-designing heat exchangers (increasing the size) can be quickly evaluated. However, the developed method did not include a way to account for the effect of changing split ratios.

By further developing the concepts used by Linnhoff and Kotjabasakis to model heat exchanger networks, a general computational tool - which can be used to evaluate the impact of changing operating conditions and operational settings on a heat exchanger network - can be developed.

1.2 Aim

This project focuses on increasing the understanding of the interaction between energy use and flexibility in the design of heat exchanger networks. The overall aim is to:

> *Investigate if the concept of Linnhoff's sensitivity tables can be used to evaluate and improve the structural flexibility and performance of large and complex heat exchanger networks by assessing design changes and operational settings under varying operating conditions.*

To emphasise the industrial relevance of this project, the heat exchanger networks at Södra Cell Mönsterås are used as a case study for investigating the viability of a rapid computational tool on an actual process. The specific project objectives are as follows:

- Develop a general MATLAB-tool for calculation of temperatures, utility duties and flowrates for any heat exchanger network.
- Propose several different retrofit designs for the heat exchanger network at Södra Cell Mönsterås for improved energy efficiency, reusing existing units as far as possible.
- Use the developed MATLAB-tool to investigate the performance of the retrofit designs during seasonal variation.
- Optimise operational settings for the retrofit designs for different seasonal conditions.
- Compare energy recovery for the different retrofit designs throughout the year.
- Validate the precision of the MATLAB-tool by comparing it to more advanced heat exchanger models.

1.3 Limitations

In order to specify a clear system boundary certain aspects will not be considered.

The MATLAB-tool is limited to handle heat exchanger networks with known UA-values, heat capacity flowrates and supply temperatures. Furthermore, it is limited to analysing the effect of changing operating conditions or settings in existing networks, but does not explicitly provide suggestions regarding specific measures to improve networks.

In terms of changing operating conditions, the MATLAB-tool is limited to handle variations in supply temperatures and heat capacity flowrates. Changes in operational settings are limited to include adjusting heat exchanger bypass ratios, network split ratios, and flowrates of non-process streams.

The network retrofit options are not formally compared from a capital cost perspective. However, a qualitative comparison is made by comparing the number of new units and their respective sizes between designs.

2
Theory

This chapter presents the general theory for the pinch analysis methodology which is used to establish energy efficiency targets for a process, and identify possible design changes to improve energy recovery within a process. Thereafter, the underlying theory behind the modelling of heat exchangers and heat exchanger networks is presented.

2.1 Pinch Analysis

This section contains a brief summary of the main concepts of Pinch analysis. A more thorough descriptions is given in [8].

The operation of industrial process plants requires liquid and gas streams to be supplied to reactors, separation units and other unit operations at specified target temperatures. In general, this implies either heating or cooling from a start temperature. A stream which requires heating is considered a cold stream and a stream which requires cooling is considered hot, regardless of the actual temperatures. If no heat exchange is performed within the process, the heating demand of all cold streams must be met by external heat sources referred to as hot utility. Similarly, the cooling demand of hot streams must be met by cold utility.

If heat is transferred from a hot stream to a cold stream, the need for cooling and heating of those streams will decrease. Consequently, the higher the level of internal heat recovery, the lower the level of utility consumption. The amount of heat recovery that is possible to achieve in a process is limited by the minimum allowed temperature difference in heat exchangers (ΔT_{min}). The smaller the temperature difference, the higher the potential level of heat recovery, but also the required heat transfer area. Thus, the choice of ΔT_{min} is a trade-off between energy recovery and capital cost for heat transfer equipment.

For a specified ΔT_{min} and a given set of hot and cold process streams, the second law of thermodynamics sets a theoretical limit for the amount of heat that can be recovered within a process. Pinch analysis is a widely used method for establishing this theoretical limit, and guide the design of a heat exchanger network which can achieve this target. Note that maximised heat recovery always means minimised hot and cold utility consumption, and pinch analysis also establishes these minima, referred to as energy targets.

In pinch analysis, energy targets are set through so called cascade calculations. Cascade calculations begin by converting actual stream temperatures into shifted temperatures. For cold streams, shifted temperatures are obtained by adding $\Delta T_{min}/2$ to actual temperatures, and for hot streams the shifted temperatures are obtained by subtracting $\Delta T_{min}/2$ from the actual temperatures. This implies that hot and cold streams with the same shifted temperature are in fact separated by ΔT_{min} and can be heat exchanged.

Table 2.1: Stream data used for the example cascade calculations in this section.

Designation	Type	$T_{start}[°C]$	$T_{target}[°C]$	CP [kW/K]
H1	Hot	170	60	3
H2	Hot	150	40	4
C1	Cold	30	150	2
C2	Cold	80	135	7

Using shifted temperatures, the process is divided into temperature intervals where the start and end points of an interval coincide with the start or target temperature of a process stream. This is illustrated in Figure 2.1 for the four streams listed in Table 2.1, using a ΔT_{min} of 10 °C. If the aggregated cooling demand of the hot streams in an interval is higher than the aggregated heating demand of the cold streams, the interval has a heat surplus. If the opposite holds, there is a heat deficit. In accordance with the second law of thermodynamics, excess heat from a high temperature interval can be cascaded to lower temperature intervals and cover a deficit there. However, low temperature excess cannot cover a high temperature deficit.

When performing cascade calculations, the excess or deficit of heat is calculated for each temperature interval. Starting at the highest temperature interval (i.e., starting from the left in Figure 2.1), cumulative excess is cascaded through the temperature intervals. If, at some interval, a deficit cannot be covered by the cumulative excess of preceding intervals, the heat flow to the next interval will be negative. This implies heat flow from lower to higher temperatures and violates the second law. In this situation, external utility will be needed. The heat cascade can be made feasible if additional heat, equal to the largest negative heat flow between intervals in the cascade, is supplied to a temperature interval above the largest negative heat flow. This removes all negative heat flow between intervals, and results in a zero heat flow between the intervals which previously had the largest negative flow.

The feasible and infeasible cascades are both visualised in Figure 2.1, where the first row gives the excess or deficit of heat in an interval, the second row gives heat flow between intervals for the infeasible cascade and the third row gives the same information for the feasible cascade. The far left number in the third and second rows represent the external heating supplied to the first interval. In general, the feasible cascade will have a cumulative excess of heat after the last interval. This must be

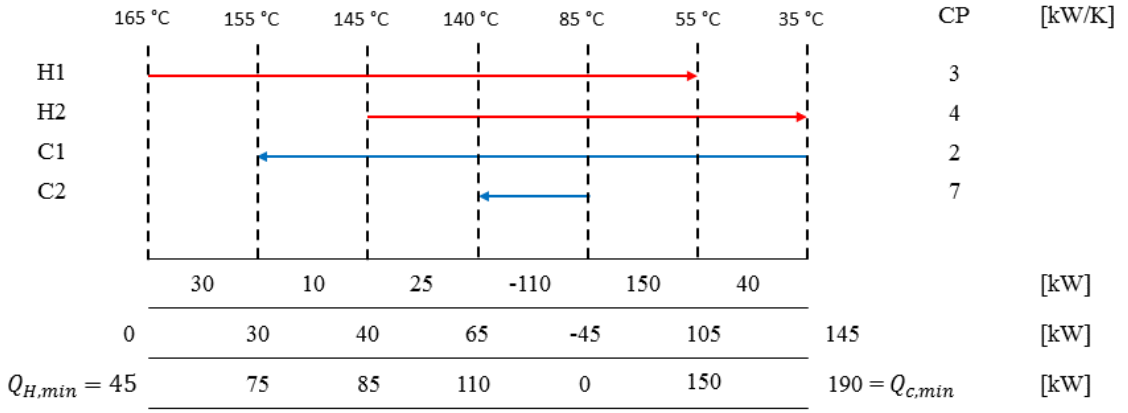

Figure 2.1: The feasible and infeasible cascades for the stream data listed in Table 2.1, using ΔT_{min}=10 °C. First row: net heat surplus or deficit in each (shifted) temperature interval. Second row: heat flows between intervals in the infeasible cascade. Third row: heat flows between intervals in the feasible cascade, and energy targets.

removed by external cold utility, and the amount is listed to the far right in the second and third rows. The amount of hot utility required to make the cascade feasible is the minimum hot utility demand of the process, $Q_{H,min}$. The corresponding excess heat after the final interval, $Q_{C,min}$, represents the minimum cooling demand.

The amount of hot and cold utility identified using the procedure outlined above are the energy targets for the process, for the specified ΔT_{min}. Note that there is no heat flow between intervals 4 and 5. The temperature (85 °C) separating the two intervals is the process *pinch point*, or pinch temperature. Above the pinch, the process has a heat deficit, and below the pinch there is an excess of heat. Since there is no heat flow between the regions above and below the pinch, the pinch can be said to divide the process into two separate parts, one with a heat surplus and one with a heat deficit. Note that the pinch temperature in the cascade is shifted. Thus, the actual pinch temperature is not the same for hot and cold streams. The pinch temperature for cold streams, the cold pinch, is obtained by subtracting $\Delta T_{min}/2$ from the shifted pinch temperature. Analogously, the hot pinch is obtained by adding $\Delta T_{min}/2$ to the shifted pinch temperature.

A commonly used graphical representation of the (feasible) heat cascade is the so-called grand composite curve (GCC), which is obtained by plotting shifted temperature against net heat flow between temperature intervals. The GCC of the four streams in Table 2.1 is shown in Figure 2.2, for a ΔT_{min} of 10 °C. Note that the choice of ΔT_{min} affects the cascade calculations, and thereby also the shape of the GCC, the energy targets and the pinch point.

As mentioned above, pinch analysis does not only identify the minimum hot and cold utility demand of a process, i.e. the energy targets, but also guides the design of heat exchanger networks which can reach the targets. Such networks are called

Maximum Energy Recovery (MER) networks. The pinch temperature is of fundamental importance for the design of a MER network, and following the three rules given below will ensure a MER network:

1. Do not use external heating below the pinch
2. Do not use external cooling above the pinch
3. Do not transfer heat through the pinch

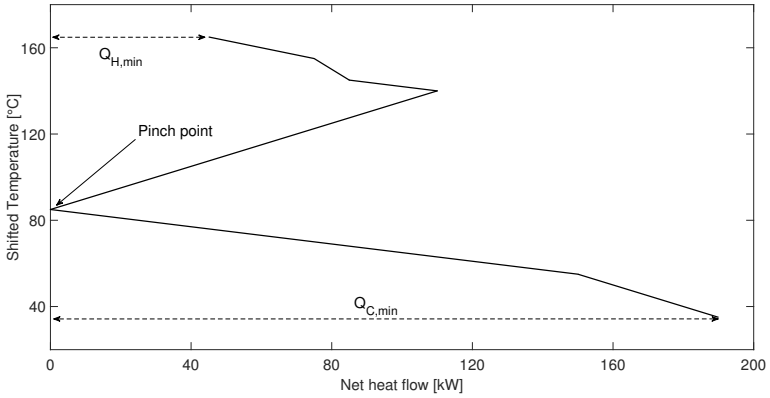

Figure 2.2: The grand composite curve (GCC) of the streams listed in Table 2.1, for ΔT_{min}=10 °C.

The first two rules relate to where utility should be used. Violating the first rule means heat is added to the region below the pinch where there is already a heat surplus, meaning more cold utility must be used. Violating the second rule means heat is extracted from the region with a heat deficit above the pinch, meaning more hot utility must be used. The third rule relates to how process streams are heat exchanged. Violating the third rule implies heat transfer from the heat deficit region above the pinch to the heat surplus region below the pinch. This means both hot and cold utility consumption will increase.

It has already been mentioned that the choice of ΔT_{min} is a trade-off between heat recovery (i.e., reduced utility costs) and equipment (capital) cost. Similar reasoning holds during network design. It is generally not economically or practically feasible to design a MER network, due to the large number of units and the complex network structures which are often needed to avoid pinch violations. The final design of the network will thus, in general, include a number of pinch violations which are considered too expensive, from a capital cost perspective, to avoid.

Beyond aiding the design of heat exchanger networks for new plants, pinch analysis can help with the much more common task of re-designing the networks at an existing plant for increased energy recovery. This task, known as retrofitting, aims at identifying and removing pinch violations in an existing heat exchanger network, and is described in more detail in Section 2.1.1.

2.1.1 Retrofit

When performing a retrofit, an existing network structure is analysed and modified. The goal of the retrofit can vary from increased energy savings to improved controllability. When performing a retrofit, the analysed network structure can be fixed or not depending on e.g. plant layout. In general, for a fixed network structure one tries to increase utility savings by identifying heat exchangers that are interconnected with the utility exchanger. From this, a sensitivity analysis can be done by increasing heat transfer area or heat transfer coefficients on the affected heat exchangers. From the analysis the most beneficial changes can be obtained for increased savings without changing anything structurally. [17]

If structural changes are allowed, one can try to work towards the MER network with the help of pinch analysis. However, it should be said that creating an MER network is often a very unrealistic goal when it comes to retrofitting since large changes in the network structure can be needed. By performing pinch analysis, existing pinch violations can be identified. The pinch violations can be removed in a stepwise procedure by re-arranging existing heat exchangers, modifying heat transfer area or by implementing new heat exchangers. For every new heat exchanger added or re-arranged cost penalties and practical constraints need to be considered. This way the retrofit changes are balanced among energy recovery and investment cost. An example of this is to remove the most critical pinch violation with the lowest cost penalty. [17]

2.2 Heat exchanger models

In the literature, several different methods for solving heat exchanger problems exist. Two commonly used methods are the "Log-mean temperature difference (LMTD) method" and the "P-NTU-method". In Linnhoff et al. [14] heat exchanger networks are solved from true counter-current heat exchanger models using the LMTD-method. Linnhoff et al. [14] derive two equations that are linear in temperature from two heat balance equations and the design equation of the LMTD-method (Equation (2.1)). The design equation uses the log-mean temperature difference, area and heat transfer coefficient to find the heat transferred, Q.

$$Q = (F)UA\Delta T_{lm} \tag{2.1}$$

When using the LMTD-method, the correction factor F (≤ 1) accounts for deviations from true counter-current flow, occurring in heat exchangers such as shell-and-tube. The P-NTU-method uses a similar approach but instead of using the design equation, the two heat balance equations are combined with an equation based on thermal effectiveness, P. This gives two equations that are linear in heat exchanger temperatures, as demonstrated in Section 2.2.1.

When comparing the two different methods, the P-NTU method is preferable for rating problems whereas the log-mean temperature method is more beneficial for

solving design problems [18]. In this work, heat exchanger network temperatures are solved for given UA-values, i.e. a rating problem. Therefore, the P-NTU method is used.

2.2.1 P-NTU method

The P-NTU method is used to model and solve rating equations for different types of heat exchangers. An overview of the model and its fundamental equations is presented below and a more detailed description about the methodology and the equations can be found in [19].

The P-NTU method uses a thermal effectiveness defined as:

$$P_h = \frac{T_{h,in} - T_{h,out}}{T_{h,in} - T_{c,in}} \tag{2.2}$$

for the hot side of the exchanger (index h for hot) and:

$$P_c = \frac{T_{c,out} - T_{c,in}}{T_{h,in} - T_{c,in}} \tag{2.3}$$

for the cold side (index c for cold). The denominator is the same for both definitions and represents the maximum possible temperature change for any of the fluids in the exchanger.

$$\Delta T_{max} = T_{h,in} - T_{c,in} \tag{2.4}$$

Using the definitions above the heat transfer between the hot and cold fluids can be expressed as

$$Q = P_h (CP)_h \Delta T_{max} = P_c (CP)_c \Delta T_{max} \tag{2.5}$$

Here, $(CP)_h$ and $(CP)_c$ are the heat capacity flowrates for the hot and cold fluid, respectively.

When solving for specific heat exchangers the thermal effectiveness can be expressed in the form

$$P_h = f(NTU_h,\ R_h,\ \textit{flow arrangement, fluid allocation}) \tag{2.6}$$

$$P_c = f(NTU_c,\ R_c,\ \textit{flow arrangement, fluid allocation}) \tag{2.7}$$

where NTU is the number of transfer units defined as the ratio $UA/(CP)_h$ for the hot fluid and $UA/(CP)_c$ for the cold fluid. R is defined as the ratio between the heat capacity flowrates according to:

$$R_h = \frac{(CP)_h}{(CP)_c} \tag{2.8}$$

$$R_c = \frac{(CP)_c}{(CP)_h} \tag{2.9}$$

Using Equations (2.8) and (2.9) combined with (2.5) gives a relationship between the thermal effectiveness of the hot and cold sides using only the heat capacity flowrate ratio.

$$P_h = P_c R_c \qquad P_c = P_h R_h \tag{2.10}$$

Using the heat balance equations for the hot and the cold side combined with corresponding expressions in Equation (2.5) gives:

$$P_h(T_{h,in} - T_{c,in}) = (T_{h,in} - T_{h,out}) \tag{2.11}$$

$$P_c(T_{h,in} - T_{c,in}) = (T_{c,out} - T_{c,in}) \tag{2.12}$$

If UA- and CP-values are assumed independent of T, Equation (2.6) and (2.7) indicate that the thermal effectiveness can be found independently of heat exchanger temperatures. Thus, under the simplifying assumption that UA- and CP-values are independent of T, Equations (2.11) and (2.12) represent two linear equations in the heat exchanger temperatures. Two examples of expressions for thermal effectiveness are presented in Appendix B for a counter-current and 1-2 shell-and-tube exchanger.

2.2.2 Heat transfer coefficients

In general, the overall U-value of a heat exchanger is related to the heat transfer coefficients of the hot and cold side fluids, and to the thermal conductivity of the material separating them. The relation is given in Equation (2.13).

$$U = \frac{1}{1/h_H + 1/h_C + 1/R} \tag{2.13}$$

Here, h_H and h_C are individual heat transfer coefficients for the hot and cold sides of the exchanger, respectively. $1/R$ describes the remaining resistance, accounting for material thickness, fouling and conductivity. For a given U-value and individual heat transfer coefficients $1/R$ can easily be solved from Equation (2.13). In the relation above, area corrections are included in the three terms in the denominator.

The individual heat transfer coefficients, h_H and h_C, vary with exchanger geometry, fluid properties and flowrates. A commonly used correlation for heat transfer coefficients (see, for example, [18]) is given by Equation (2.14) which is valid for non-viscous liquids in the turbulent flow regime:

$$h_i = 0.023 \frac{k_f}{d} Re^{0.8} Pr^r \tag{2.14}$$

Here, i is either H for hot or C for cold. k_f is the thermal conductivity of the fluid, d is a characteristic length representing heat exchanger geometry, Re is the Reynolds number and Pr is the Prandtl number. The index, r, for the Prandtl number is generally taken as 0.3 for cooling and 0.4 for heating. For a given heat exchanger, d is constant and if fluid properties are assumed independent of temperature, Equation (2.14) can be reduced to

$$h_i \propto f_i^{0.8} \tag{2.15}$$

where f is fluid flowrate. If the heat transfer coefficient is known for a certain design flowrate, the heat transfer coefficient at a new flowrate can thus be estimated according to

$$h_{new} = \left(\frac{f_{new}}{f_{design}}\right)^{0.8} h_{design} \tag{2.16}$$

For the design condition, Equation (2.13) can be rewritten as

$$U_{design} = \frac{h_{H,design}}{1 + \frac{h_{H,design}}{h_{C,design}} + \frac{h_{H,design}}{R}} \tag{2.17}$$

By combining this expression with Equation (2.16), the U-value at the new flowrate can be estimated by

$$U_{new} = \frac{h_{H,design}}{\left(\frac{f_{H,design}}{f_{H,new}}\right)^{0.8} + \frac{h_{H,design}}{h_{C,design}}\left(\frac{f_{C,design}}{f_{C,new}}\right)^{0.8} + \frac{h_{H,design}}{R}} \tag{2.18}$$

The U-value at a new flowrate can now be related to the U-value at the design flowrate according to

$$U_{new} = \underbrace{\frac{1 + \frac{h_{H,design}}{h_{C,design}} + \frac{h_{H,design}}{R}}{\left(\frac{f_{H,design}}{f_{H,new}}\right)^{0.8} + \frac{h_{H,design}}{h_{C,design}}\left(\frac{f_{C,design}}{f_{C,new}}\right)^{0.8} + \frac{h_{H,design}}{R}}}_{\text{Correction factor}} \times U_{design} \tag{2.19}$$

Under the simplifying assumption that fluid properties are independent of T, Equation (2.19) can be used to estimate the effect that changing flowrates have on the UA-value of a heat exchanger. The scaling factor in Equation (2.19) will in the following be referred to as a correction factor used to correct the design UA-value for deviations from design flows.

2.3 Heat exchanger network equations

This section establishes the number of unknown temperatures in a general heat exchanger network, and the equations used to solve them. A similar derivation is given in [17]. An illustration of a simple heat exchanger network is given in Figure 2.3. To solve this network, all unknown temperatures must be calculated. During the calculations, heat capacity flowrates and temperatures are known for all supply streams. The same applies for heat exchanger UA-values and flow arrangements. This means all required data for the P-NTU method is known and as demonstrated in Section 2.2.1, two linear equations in T can be obtained for each heat exchanger in the network. Thus, a network with n_E heat exchangers gives $2n_E$ linear equations.

Using Figure 2.3 it can be verified that a stream with no heat exchangers has a constant temperature (for the entire stream), and that one additional temperature is added for each heat exchanger added to the stream. Since each exchanger is

connected to one hot and one cold stream, there will be two additional temperatures for each exchanger added to the network. A system with N streams and n_E heat exchangers will therefore have N temperatures for the streams themselves, and $2n_E$ additional temperatures for the heat exchangers, yielding a total of $N + 2n_E$ temperatures. If the N supply temperatures are known, there are $2n_E$ unknown temperatures. Using the $2n_E$ equations obtained for the heat exchangers, a linear equation system can be obtained and solved for all temperatures in the network.

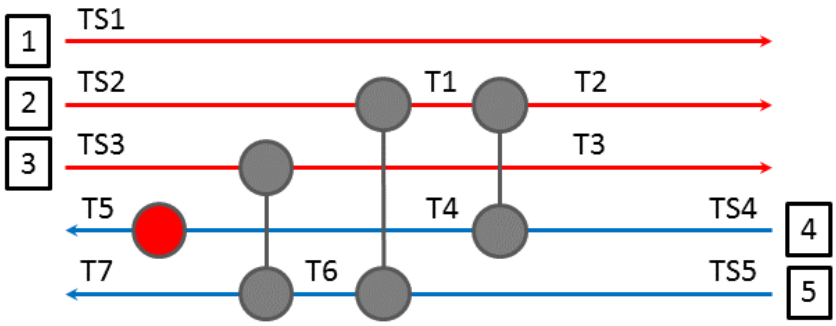

Figure 2.3: Numbering of network temperatures in an example heat exchanger network. This network has 5 supply temperatures (TS1-TS5) and 7 additional network temperatures (T1-T7), giving 12 temperature nodes in total.

In Figure 2.3, stream number 4 is equipped with one utility exchanger. The actual utility stream is not included in the network and, as stated above, each utility adds an extra unknown temperature to the stream it is placed on. An additional equation is also obtained for the stream in question via a heat balance over the utility:

$$Q_{utility} = CP\Delta T$$

If heat loads ($Q_{utility}$) are given for all utility exchangers, each such exchanger generates an additional linear equation in T. Alternatively, the outlet temperature of the exchanger can be specified directly. This gives a trivial equation where the extra unknown network temperature is set equal to a constant (the specified outlet temperature).

In conclusion, a heat exchanger network with N streams, n_E heat exchangers and n_U utilities will have $N+2n_E+n_U$ temperatures. If supply temperatures are specified for each stream, the number of unknowns are $2n_E + n_U$. If CP-values are given for each stream, and UA-values and flow arrangements are given for each process-to-process exchanger, $2n_E$ linear equations in T can be obtained via the P-NTU method. If heat loads or outlet temperatures are given for each utility exchanger, n_U additional linear equations are obtained. This gives a total of $2n_E + n_U$ linear equations and all network temperatures can be calculated by solving the resulting system of equations.

Note that if given CP-values differ from design values, the exchanger UA-values can be updated using equation 2.19 before solving the network temperatures.

2.3.1 Stream splitting and mixing

In the preceding discussion, stream splitting or mixing were not considered. However, if stream splitting or mixing are included, it is not sufficient to consider only the heat balance; the mass balance must be considered as well. Below, splitting of a single stream into two branches is considered and each stream split is treated as generating two new streams, with unknown CP-values and start temperatures. This is illustrated in Figure 2.4. If all supply stream CP-values are known, a network with n_S splits has $2n_S$ unknown CP-values. Using only mass balances for the splits (a total of n_S equations), leaves one degree of freedom per split. However, if split ratios are defined for each split, all CP-values in a network are well-defined and can be calculated. Since CP-values are considered independent of temperature, they can be calculated before solving for network temperatures.

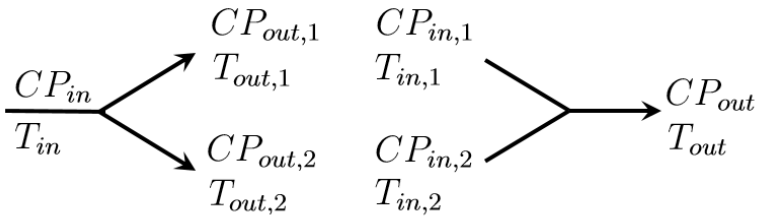

Figure 2.4: An example of stream splitting (left) and stream mixing (right), illustrating the known inlet and unknown outlet parameters of the two operations.

Since the outlet temperatures from the split are unknown, each stream split gives two additional unknown temperatures. However, two additional equations are also obtained; one from the heat balance and one from the fact that the two outlet temperatures are equal. In this work, all splits are considered adiabatic. This leaves two trivial equations for the unknown temperatures:

$$T_{out,1} = T_{in}$$
$$T_{out,2} = T_{in}$$

Thus, stream splitting gives two additional temperatures and two additional linear equations in T meaning all unknown temperatures can still be calculated by solving a linear equation system. Prior to solving for the temperatures, CP-values of the split streams can be found given that all split ratios are defined.

For stream mixing, the situation is similar. Each mixing is treated as giving one new stream with unknown CP and start temperature. Each mixing also gives an additional mass balance and the new CP can be calculated prior to solving for network temperatures, if CP-values are considered independent of T.

The unknown start temperature resulting from mixing means each mixing point gives one additional temperature. However, one additional linear equation in T is

obtained via the heat balance for ideal mixing:

$$T_{out} = \frac{CP_{in,1}T_{in,1} + CP_{in,2}T_{in,2}}{CP_{out}}$$

Including mixing therefore gives as many new linear equations in T as it gives unknowns, and network temperatures can still be solved using a linear equation system.

Note that after the network mass balance is solved, the correction factor in Equation (2.19) can be used to update UA-values for deviations from design flowrates, before solving for network temperatures.

2.4 Sensitivity tables

The methodology of 'Sensitivity tables', mentioned in Section 1.1, was introduced by Linnhoff et al. [14] to provide a quick way of estimating the passive response of a HEN to changing operating conditions, and to identify options to mitigate an unwanted response [14]. In this context, changes in operating conditions are variations in heat capacity flowrates or supply temperatures of streams in the HEN. In the work of Linnhoff et al., mitigating options are changes in UA-values of exchangers, and can be either in terms of increasing the UA-value (a design change) or decreasing the UA-value by partial bypass, i.e. a change in operational settings. In this work, mitigating options also include the possibility of adjusting split ratios. The sensitivity tables list the sensitivity of network temperatures to changes in UA-values, supply temperatures, CP-values or split ratios. For a given change in operating conditions or operational settings, the tables allow estimating the resulting effect on network temperatures.

To generate sensitivity tables, all temperatures in the HEN are first calculated for the base case, i.e. a case when all supply temperatures, CP-values, UA-values and split ratios are at their initial design points. Next, the value of one parameter of interest (e.g., the CP of stream i) is adjusted from its base case value, and all network temperatures are calculated again and compared to the base case values. In this way, the sensitivity of network temperatures to changes in that parameter can be found. The results are collected in a sensitivity table for the investigated parameter.

The resulting tables will have the same overall structure for UA-values, CP-values and split ratios. However, the table for supply temperatures represents a special (simplified) case. This is due to the fact that the equations used to represent the HEN are linear in the network temperatures, as described in Section 2.3.

In the sensitivity table for supply temperatures, each column represents variations in one supply stream temperature. The supply temperature is changed with +1 °C and the effect of that change on all unknown network temperatures is seen in the corresponding column. Due to the temperature linearity, the effect of larger or smaller changes can be evaluated by multiplication of the table entries. For example, the effect of a 10 °C change in a supply temperature is obtained by multiplying the

values in the corresponding column by 10. Note that in some cases this can lead to non-feasible conditions. An example of a sensitivity table for supply temperatures is seen in Table 2.2.

Table 2.2: Sensitivity Table for an arbitrary heat exchanger network with three supply temperatures, $TS_1 - TS_3$. The table lists changes in network temperatures $T_1 - T_4$ resulting from 1 °C change in supply temperatures $TS_1 - TS_3$. Example of use: if TS_2 increases by 12 °C, T_3 decreases by $12 \times -0.5 = -6$°C.

	TS_1	TS_2	TS_3
T_1	1.5	-0.5	0.2
T_2	2	-0.8	0.5
T_3	1	-0.5	-0.3
T_4	-1	0.2	-0.1

Changes in split ratios, CP- and UA-values have a non-linear effect on network temperatures. Therefore, it is not sufficient to evaluate the effect of one level of change and obtain the effect of other levels of change by multiplication. This means a range of values must be evaluated for each investigated parameter (a split ratio, CP- or UA-value). Consequently, one table (not just one column, as was done for supply temperatures) is created for every stream (CP), heat exchanger (UA) or split ratio that is investigated. Each column represents a level of change from the base case value. An example of a sensitivity table for UA is given in Table 2.3.

Table 2.3: Sensitivity Table for UA_1 in an arbitrary heat exchanger network. Example of use: if the UA-value of exchanger 1 is reduced 20 % from its base case value, network temperature T_1 decreases by 1 °C.

	-20 %	-10%	0	+10 %	+20 %
T_1	-1	-0.2	0	+0.3	+0.5
T_2	-1.4	-1	0	+0.6	+1.5
T_3	+3	+1.2	0	-0.7	-2.3
T_4	+2.2	+0.9	0	-0.1	-0.3

Linnhoff et al. [14] generated sensitivity tables for CP without updating UA-values to account for the changing flowrates. In this work, the correction factor in Equation (2.19) can be used to correct UA-values when generating tables for CP-values and split ratios.

Once generated, the tables are used in the following way: the sensitivity tables for supply temperatures and CP-values are used to estimate the effect of variations in these parameters. If the variations cause network temperatures to reach unacceptable values, the UA-tables and the split ratio tables are used to maintain target temperatures. During this procedure, table entries relating to different parameter variations are added together to estimate the effect resulting from simultaneous

changes.

Note that each column in the sensitivity tables represents an *exact* solution to the linear equation system describing the heat exchanger network, for the parameter variation associated with that column. However, if entries from different tables are combined in the way described above, the resulting value no longer represents an exact solution to the HEN equation system with respect to the parameter variations from which the table entries derive. This is because each table is generated with all other operating and design parameters reset to their base case values. Since the heat exchanger equations are neither linear in CP and UA-values, nor in split ratios, linear addition of the result from individual variations will not give the exact result of simultaneous variations.

To obtain the exact HEN temperatures resulting from simultaneous variations in network conditions, the equation system can instead be solved with the new set of operating and design data. With modern computational power, solving the required equation system is simple. With a program that allows the designer to change HEN parameters in a straightforward way, the effect of simultaneous variations can be calculated by solving the updated equation system rather than by adding table entries. This approach is both faster and more accurate.

With modern computational power, the result of simultaneous variations is easily calculated and doing estimations using the sensitivity tables is obsolete. However, the tables are still useful for screening of design changes, or changes in operational settings, to improve network performance during varying operating conditions.

3
Methodology

The methodology chapter describes the work procedure. The project is divided into two main areas which are interconnected. The work begins with the development of a MATLAB-tool for steady-state heat exchanger network calculations. The MATLAB-tool also has the possibility to generate user-specified sensitivity tables for design parameters and operational settings. The design process of the program is described in Section 3.1. The MATLAB-tool is then used to assist the next step, which involves a case study performed at Södra Cell Mönsterås pulp mill. In the case study, retrofit proposals are produced where the MATLAB-tool is used to guide improvements and evaluate the effect of seasonal variations in operating conditions. More details on the network design procedure are given in Section 3.2.

3.1 MATLAB-tool for HEN calculations

The first part of the project includes the development of a general tool in MATLAB for analysis of heat exchanger networks and generation of sensitivity tables. The goal is to develop a script with user-friendly data input and a quick computational time which can solve any type of network. Apart from defining any network structure, the user can also choose from a set of predefined heat exchanger types to be used in the network. Different heat exchangers common in industry were identified through a literature study and are presented in Chapter 4. In the program, the P-NTU method using thermal effectiveness is used to model and represent the different heat exchangers, see Section 2.2.1.

During the development of the MATLAB-tool, continuous testing was performed to validate the network solver, user-input method and detect bugs and errors. While testing the program on smaller heat exchanger networks it is possible to verify the results by hand or double check with simple examples from the literature. Furthermore, when testing large and complex example networks, the solver is validated by making sure that changes in operating parameters are correctly propagated throughout the system. Thereafter, a validation process of the correction factor, Equation (2.19), was performed and is explained in Section 3.1.1. An overview of the work procedure for the development of the MATLAB-tool is summarised in Figure 3.1.

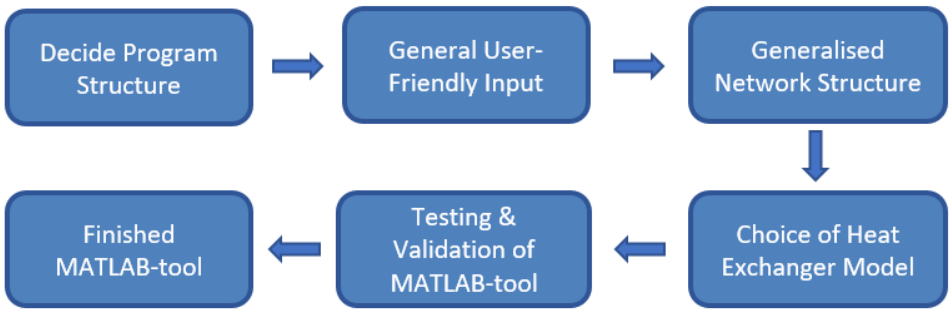

Figure 3.1: Work procedure for the development of the MATLAB-tool.

3.1.1 Validation of MATLAB-tool

In the MATLAB-tool, the heat exchangers are modelled from a specification case where UA-values are calculated for given conditions. The MATLAB-tool provides an exact solution to the network mass balance and for given UA-values, flowrates and split ratios, the calculated network temperatures are exact. However, the accuracy of the correction factor for new flowrate conditions as defined in Equation (2.19) is uncertain. This correction factor is used to update exchanger UA-values for flowrate deviations from a given specification point at which the UA-value and individual heat transfer coefficients are known. To validate the correction factor, the precision and performance of the MATLAB-tool is compared to a model developed by mill engineers at Södra Cell Mönsterås. The model involves a similar subsystem of the mill's heat exchanger network as the one investigated in the case study, explained in Chapter 5, and calculates network temperatures for a given set of operating conditions. The heat exchanger models account for flowrates, exchanger geometry and temperature dependencies of fluid properties. The Södra-model also calculates the individual heat transfer coefficients for a specific heat exchanger for a given set of operating conditions.

To perform the validation, the design data needed to calculate the correction factors for the different heat exchangers was obtained from the Södra model for a specification case corresponding to springtime operating conditions. The UA-values of the heat exchangers in the MATLAB-tool will, by definition for this case, match the values in the Södra-model. From this, typical summer and winter conditions are used as input for both the Södra-model and the MATLAB-tool, with or without correction factor. The Södra-model is used as a reference since it re-calculates the overall heat transfer coefficients for the new set of operating conditions. The impact on network temperatures and UA-values for the MATLAB-tool, with and without the correction factor, are compared to the new values obtained from the Södra-model. Taken together, the validation process provide new information regarding the precision of the MATLAB-tool when evaluating heat exchanger networks with changing operating conditions, see Section 6.5.

3.2 Case study - Södra Cell Mönsterås

To demonstrate the usefulness of the MATLAB-tool in a real industrial application, a case study was carried out on the heat exchanger networks of a large Kraft pulp mill, Södra Cell Mönsterås, which is described in Chapter 5. The case study includes a pinch analysis of the mill, see Section 5.4, which identifies energy targets and pinch violations for spring conditions. The existing network design is at first retrofitted using spring conditions without the MATLAB-tool to specify the dimensioning of new and existing heat exchangers. By using the specified dimensions additional designs are developed which represent variations of the first retrofit. The different retrofit proposals are then with the help of the MATLAB-tool evaluated and improved for different seasonal conditions. Thus, the MATLAB-tool gives a good overview of the expected performance over a year. The work process for the development of retrofit proposals is presented in Figure 3.2.

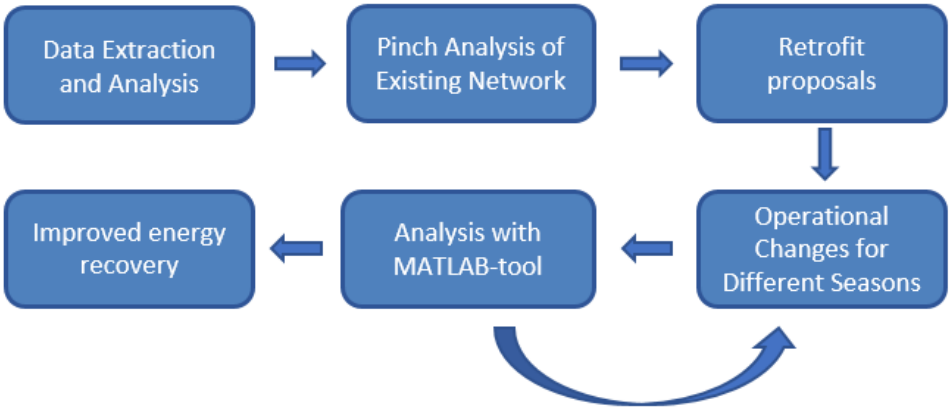

Figure 3.2: Flowsheet of the work process of the retrofitted heat exchanger networks.

3.2.1 Data extraction and analysis

The energy systems and heat exchanger networks of Södra Cell Mönsterås were mapped by Nihlmark and Mahmoud in a previous Master Thesis [7]. The resulting stream and flow data lay the foundation for this case study. The data set extracted by Nihlmark and Mahmoud is valid for a high production rate of softwood pulp during spring conditions. This data set is analysed in Aspen Energy Analyzer which is a commercial software used to perform pinch analysis.

The work done by Nihlmark and Mahmoud reflects spring conditions. However, in order to analyse the flexibility and performance of the different retrofits for variations, additional operational data is extracted for winter and summer conditions from Södras' process monitoring system. By doing this, a better estimation can be achieved regarding the network response and energy recovery throughout the year. The data is extracted during full production and during production of softwood pulp, as for springtime operation, in order to give a fair comparison between

the seasons. A more thorough walkthrough of the data extraction and analysis is presented in Sections 5.3 - 5.5.

3.2.2 Retrofit procedure

In order to identify retrofit options, a pinch analysis is performed on the extracted data set. By consulting mill engineers at Södra Cell Mönsterås, hard and soft target temperatures are identified. Streams that must reach their targets (hard) are distinguished from streams for which some lee-way exists (soft). Energy targets and pinch temperatures are determined with Aspen Energy Analyzer.

Based on the results from the pinch analysis, a sub-network of the entire heat exchanger network is selected for further analysis. Based on the performed pinch analysis for spring conditions, this sub-network is retrofitted by hand, yielding a base case retrofit design which is explained in detail in Section 6.3.2. This base case is used to specify the dimensioning of new and existing heat exchangers with the purpose of minimizing the effect of the retrofit actions on the rest of the system. This is achieved by introducing constraints on a number of temperatures. The system boundary of the base case network is then enlarged to include more subsystems. The interconnections among these subsystems and the subsystem chosen initially can be analysed using the MATLAB-tool. The tool enables the user to change the position of heat exchangers or their UA-value and still keep track of all temperature changes within the system. From this, different design proposals are developed which are presented in detail in Section 6.4.1. The different design proposals are evaluated for different seasons where a new set of operating conditions, different from those used during the first retrofit, are obtained from Södra Mönsterås' process monitoring systems. The retrofits are further improved with special attention to changes in split ratios and flowrates which open up for greater total energy savings. The correction factor included in the MATLAB-tool update the UA-values when changing operating conditions or for example split ratios.

During the design process, the MATLAB-tool is used to assess the networks' response to the new operating conditions. In an iterative process, the MATLAB-tool provides a quick overview of the different measures needed to counteract variations and improve the network for changing conditions. Considering the simulation speed of the MATLAB-tool, design and operational changes can easily be manually investigated and derived. The MATLAB-tool also gives the possibility to derive sensitivity tables where changes of flows, UA-values, temperatures and split ratios can be analysed in terms of downstream changes of temperature. The design process does not only give a more energy efficient network, compared to the base case retrofit, but in the end also serves as a demonstration of the usability of the developed MATLAB-tool. The interconnection is visualised in Figure 3.2.

4

MATLAB-tool

In this chapter the functions and required inputs of the developed MATLAB-tool are presented. A validation of the correction factor described in Section 2.2.2 and used by the MATLAB-tool to update UA-values is presented in Section 6.5. The impact of the correction factor on the final retrofit proposal, seen in Section 6.4.2, is demonstrated in Section 6.5.2.

The created tool requires a combination of heat exchanger network implementation in Excel and calculations performed in MATLAB. Identifying heat exchanger networks as grid systems implies that any type of network can be interpreted and calculated using the MATLAB-tool. The MATLAB-tool calculates all temperatures, flowrates and duties in a heat exchanger network for a given set of base operating conditions. This also includes more advanced network layouts with re-circulating flows and streams which alternate between being hot and cold. The following input is needed for a complete run.

For each process-to-process heat exchanger:

- UA-value
- Type of heat exchanger
- Hot and cold stream ID
- Position on hot and cold stream
- Individual heat transfer coefficients and CP-values (Correction factor)

For each supply stream:

- CP-value (Hot or cold)
- Temperature

For each split/mix:

- Inlet and outlet stream ID
- Split ratios

In addition to solving all the temperatures, flowrates and duties in a network, the program can generate sensitivity tables. For user specified variations in operating conditions, it calculates the resulting changes. In this way, the sensitivity of network temperatures to changes in a given process parameter is found. The results are collected in a sensitivity table for the investigated parameter.

The MATLAB-tool generates sensitivity tables for:

- Supply temperatures
- CP-values of streams

- UA-values of heat exchangers
- Split ratios

The program performs the heat exchanger calculations with the help of the P-NTU method described in Section 2.2.1. In the literature [19] several different heat exchanger models exist whereas only a few are implemented in the MATLAB-tool.

The MATLAB-tool handles calculations for the following heat exchangers:

- True counter-current heat exchangers
- Parallel flow heat exchangers
- External utility heat exchangers - hot and cold
- Shell-and-tube heat exchangers
- Plate-and-frame heat exchangers

The user has the possibility to add additional heat exchangers given that existing data for its thermal effectiveness, P, exists. More in depth information about the usability and possibilities of the program is documented in an external user manual, "HEN-S - User Manual" [20]. The user manual also provides some hands-on examples of usage and network implementations.

5

Case Study - Background

The case study included in this work represents an industrial case of a Kraft pulp mill. The purpose is to demonstrate the usefulness of the developed MATLAB-tool as an aid in the design process of complex heat exchanger networks. Below, the MATLAB-tool is used to guide the retrofit design of the heat exchanger networks for the Kraft pulp mill Södra Cell Mönsterås. A brief description of the studied system is given in Section 5.2 along with the aim of the new network design. Details on stream selection and data extraction are presented in Section 5.3 and 5.5 and the current energy situation of the mill is outlined in Section 5.4 by presenting the current energy use, the pinch temperature, the GCC and energy targets. In Section 6.4, the network design procedure, using the MATLAB-tool, is presented in more detail along with the resulting heat exchanger networks.

5.1 The Kraft pulp process

This section gives a brief overview of the pulping process used at Södra Cell Mönsterås, adapted from [7]. Pulp is the feedstock in papermaking and consists of cellulose fibres from wood, fibre crops or similar. At Södra Cell Mönsterås, pulp is produced either from hard- or softwood using the Kraft process. The Kraft process is a chemical pulping process, meaning the cellulose fibres are extracted from the wood by chemical rather than mechanical means. Specifically, the Kraft process uses a solution of sodium hydroxide and sodium sulphide, called white liquor, to dissolve the lignin which binds cellulose together in the wood. A schematic overview of a Kraft pulp mill is seen in Figure 5.1.

After arriving at the mill, wood logs are debarked and cut into chips. The bark is sent to a bark boiler for heat and power generation, while the wood chips are sent to the mill's digester section. Here, the wood chips are mixed with white liquor and cooked in three continuous digesters at temperatures around 165 °C. This process separates the cellulose fibres by dissolving the lignin which binds them together. The pulp - i.e., the separated cellulose fibres - is screened and washed to remove impurities. The screened and washed pulp is bleached in several stages using various chemicals. The bleaching process makes extensive use of process water for washing out bleaching chemicals. After bleaching, the pulp mixture is 99 % water by weight and must be dried to reach a dry solids content of about 90 %. The drying is the final treatment of the pulp, after which sellable pulp is obtained.

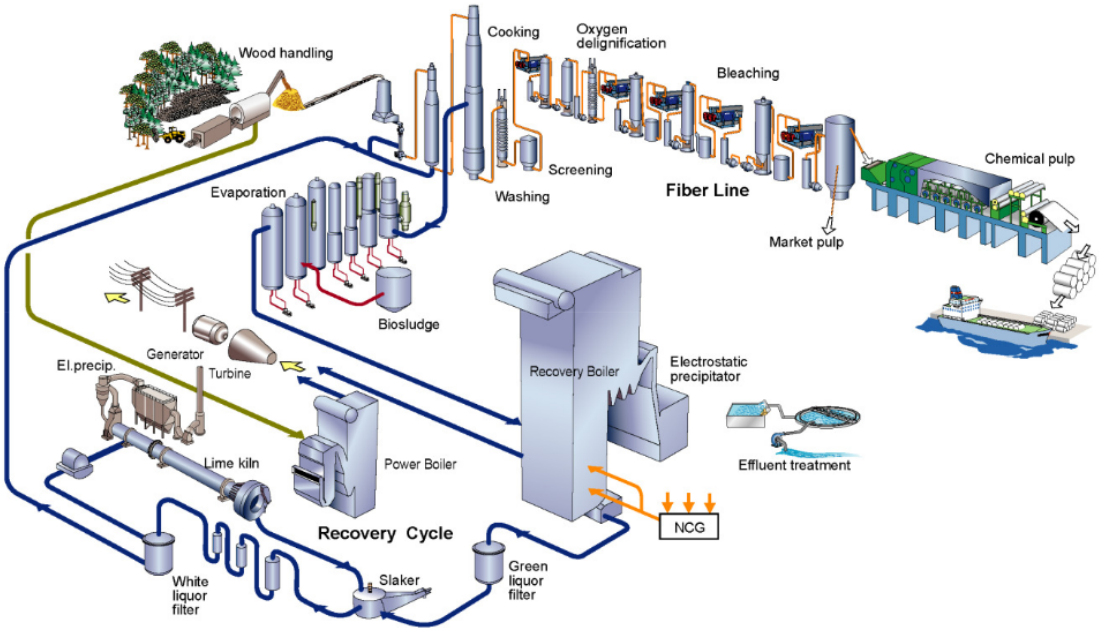

Figure 5.1: General overview of a Kraft Pulp mill [21].

During cooking in the digester, the lignin content of the wood ends up in a solution called black liquor which also contains spent cooking chemicals. The black liquor is washed from the pulp mixture in the digester and subsequently flashed in two stages. Parts of the condensate from the first flash is sent back to the digester for use in the cooking process, while the rest is sent to a second flash. The condensate from this second flash is called thin black liquor. The flash vapour is condensed and the resulting condensate is used for turpentine production.

The dilute black liquor leaving the second flash is cooled and sent to the mill's evaporation section. Through evaporation, the dry solids content of the dilute liquor is increased from about 15 % to about 78 %, yielding thick black liquor. The higher solids content allows the thick black liquor to be combusted in a so-called recovery boiler. The main purpose of this boiler is to recover cooking chemicals from the black liquor, a step that is necessary for economic operation of the mill. The combustion of black liquor forms a melt which, after being discharged from the boiler, is mixed with water to generate green liquor. Green liquor is then mixed with lime (calcium oxide) to regenerate white liquor.

While one of the purposes of the recovery boiler is to regenerate cooking chemicals from the thick black liquor, it is also very important for the mill's energy systems. In fact, the steam generation in the recovery and bark boilers (of which the recovery boiler is the larger one), is enough not only to cover the process demand of steam, but also to produce an excess of heat and power. Södra Cell Mönsterås is a net exporter of electricity and the excess heat is used for district heating. Three separate heating networks are supported by the mill. These are for heating the mill premises

(internal heating network), for delivering heat to the nearby sawmill (sawmill heating network) and for district heating to the municipality of Mönsterås (external heating network).

5.2 Studied system and retrofitting aim

Södra Cell Mönsterås is a large kraft pulp mill with an annual production capacity of 750 000 air dried tons. The mill's heat recovery is achieved mainly through a secondary heating system (SHS). This system is a circulating water network which is used for both cooling and heating of process streams. Make-up water enters the system from the nearby river Emån and is heated by heat exchange with hot process streams. The resulting heated water can then be used to heat cold process streams. Thus, the secondary heating system represents a way of indirect heat exchange between process streams. Besides this, the pulping process itself requires water at certain temperatures. This means water is not only used as a heat transfer media, but is also used directly in the process.

The secondary heating system has three interconnected main temperature levels: cold water (CW) at 15 °C, warm water (WW) at 55 °C and hot water (HW) at 85 °C. Water is heated or cooled to the different levels by heat exchange with process streams and for each temperature level, a storage tank exists to balance fluctuations in production and consumption. A good overview of the secondary heating system at Södra Cell Mönsterås is given by Nihlmark and Mahmoud [7].

Since the highest temperatures in the secondary heating system are about 85 °C (the highest tank temperature) indirect heat exchange via the secondary heating system can provide heating only to temperatures slightly below 85 °C. Consequently, if a process stream requires heating to higher temperatures it must be heat exchanged directly with hotter process streams or heated with steam. If the temperatures in the secondary heating system are increased, it will be possible to use indirect heat exchange at higher temperatures.

In the case study, the steam demand for heating of process streams is reduced either by improved process-to-process heat exchange or by producing secondary heating water at higher temperatures, thus allowing higher temperatures in indirect heat exchange. Consequently, design changes are made involving the secondary heating system. When such design changes are made, it must be ensured that the total amount of hot and warm water produced in the secondary heating system is still sufficient to meet the consumption. This includes both the demand for hot and warm water for heating of process streams, a demand that may change due to the retrofits, and the demand of warm and hot water for direct use in the process. The latter includes those parts of the pulping process where water at certain temperatures is needed in the process, for example for washing or dilution. This water must always be produced, no matter what changes are made to the energy recovery systems of the mill.

For the purpose of pinch analysis, all demands of water for actual use in the process are aggregated into process streams with target temperatures equal to the temperature where the water is used. Some sections of the mill, for example the bleaching section, have not been mapped and are treated as black boxes. Any water from the secondary heating system entering such sections is also treated as a process demand since the actual use of the water is unknown. No other water streams in the secondary heating system are included in the pinch analysis since they only represent a way of indirect heat transfer between process streams and are not in themselves a process demand. However, it must still be ascertained during network design that the amount of hot and warm water produced matches both the demand of the process and for heating of process streams.

5.3 Stream selection

In 2017, Nihlmark and Mahmoud [7] mapped the energy systems at Södra Cell Mönsterås with special focus on the plant's secondary heating system. During the mapping, the mill was operating at a high production rate of softwood pulp at spring conditions. Consequently, the established process parameters are valid only during these conditions while the established layout of the secondary heating system is valid at any time. The mapping include a pinch analysis of the mill, with more details specified for the parts connected to the secondary heating system.

The hot and cold streams included in this case study are to a large extent based on the stream definitions made by Nihlmark and Mahmoud [7]. However, some changes in stream definitions are made to better suit the purposes of this work. Nihlmark and Mahmoud made some stream definitions which were heavily influenced by the current layout of the plant. While this gives a correct view of the current and minimum energy use at the mill, it limits the possibilites to identify improvements to the design. For the stream data used in the case study of this work, the stream definitions made by Nihlmark and Mahmoud are used as a starting point. Piping and instrumentation diagrams of the mill were consulted in order to decouple the stream data from the current plant layout and to identify data inconsistencies.

Regarding the process demand of water, Nihlmark and Mahmoud included three temperature levels; 55 °C, 85 °C and 90 °C. The temperature levels have been maintained but the amount of water needed at the different temperatures was not sufficiently documented. Therefore, the amounts of water needed at the three different temperatures have been re-estimated in co-operation with mill engineers at Södra Cell Mönsterås.

All parts of the process below the cold tank temperature (15 °C) are ignored, because of insufficient mapping and the fact that no significant energy savings are probable at such low temperatures. This means cold water is assumed to be available at the cold tank temperature and no investigation is made regarding how the water reaches this temperature from the intake (river) temperature. Consequently, the starting

temperature of all cold streams representing a process demand of water is chosen to be 15 °C.

5.4 Targeting and performance

The results from the data extraction are presented as hot and cold streams in two tables. Table 5.1 presents the hot streams used for the case study whereas cold streams are presented in Table 5.2. The largest difference with the updated stream tables compared to Nihlmark and Mahmoud is an additional heating demand of feed water of 51 MW in the cold table. However, this is partly met by a hot stream from a steam condensate tank representing 33.7 MW. More information about all changes made to the established stream data by Nihlmark and Mahmoud are documented in Appendix A. The changes include modifications such as merged streams and updated values.

Table 5.1: The hot stream data representing the entire mill for spring conditions.

Stream	Description	Media -	Phase -	T_{start} [°C]	T_{target} [°C]	F [kg/s]	CP [MW/K]	Q [MW]
H1	Steam condensation 1st evaporation section surface condenser	Steam	Condensing	65	65	-	-	30.73
H2	Steam condensation 2nd evaporation section surface condenser	Steam	Condensing	65	65	-	-	73.67
H3	Cooling of oxygen liquor for use in bleaching	Oxygen liquor	Liquid	94	84.4	114.6	0.479	4.6
H4	Cooling of liquor tank	Oxygen liquor	Liquid	94	88.6	149.7	0.648	3.5
H5	Cooling demand of mist condensers for the recovery boiler	Water	Liquid	86.2	59.2	-	-	15.0
H6	Liquor condensate from evaporation section 1&2	Water	Liquid	83.4	15	221.7	0.927	63.4
H7	Thin liquor to Tank 1/2	Thin liquor	Liquid	112.94	95.6	257.9	1.078	18.7
H8	PO-gas used as heat source	Moist air	Moist	100	95.8	-	0.575	2.4
H9	BSO to process	Water	Liquid	89.7	86.4	-	0.367	1.21
H10	Cooling of BSO tank	Water	Liquid	89.7	88.5	-	-	0.1
H11	Fimp coolers K4 & K5 - Digester section	Liquor (LTV)	Liquor	132.7	114	-	0.214	4
H12	Flash steam and saw mill condenser - Digester section	Degassed Turpentine	Condensing	110.9	110.9	-	-	14.69
H13	Primary turpentine condenser - Digester section	Degassed Turpentine	Condensing	112.6	112.6	-	-	5.15
H14	Turpentine condenser K6 - Digester section	Degassed Turpentine	Turpentine	98.7	98.7	-	-	1.56
H15	Condenser for uncondensed turpentine	Degassed Turpentine	Turpentine	104	104	-	-	7.04
H16	Cooler turpentine - Digester section	Turpentine condensate	Liquid	102.1	81.6	-	0.029	0.58
H17	Liquor cooler - Digester section	Water	Liquid	95.4	67.2	16	0.055	1.56
H18	BQ1 backwater	Water	Liquid	86.7	40	355.67	1.487	69.4
H19	Cooling of BPO tank	Water	Liquid	93	86.5	96.3	0.402	2.6
H20	Flue gas released from recovery boiler	-	Gaseous	197	140	188.4	0.188	10.74
H21	Moist air from drying section blown out to atmosphere	Moist air	Moist	56	30	113.3	-	30.90
H22	VVX 16 - Heating demand feed water	Water	Liquid	100.6	31.4	116.49	0.487	33.70

Based on the hot and cold stream data given in Tables 5.1 and 5.2 the process GCC in Figure 5.2 was obtained using Aspen Energy Analyzer, using a global ΔT_{min} of 10 °C. The shifted pinch temperature of the obtained GCC is 107.5 °C. It should be noted that when performing a sensitivity analysis, the pinch is sensitive to an increase in ΔT_{min}. For ΔT_{min} of 13.2 °C the pinch changes to

Table 5.2: The cold stream data representing the entire mill for spring conditions.

Stream	Description	Media	Phase	T_{Start} [°C]	T_{Target} [°C]	F [kg/s]	CP [MW/K]	Q [MW]
C1	Feed water heating - Condensate	Water	Liquid	31.4	125	116.5	0.487	45.58
C2	Feed water heating - make up	Water	Liquid	8.3	125	63.3	0.265	30.88
C3	Air preheating	Air	Gaseous	32.7	164.8	154.4	0.155	20.41
C4	Sawmill heating network	Water	Liquid	59	105	140	0.585	26.92
C5	Process demand of warm water	Water	Liquid	15	55	573.6	2.404	96.14
C6	Process demand of hot water	Water	Liquid	55	85	455	1.902	57.06
C7	Process demand of hotter water	Water	Liquid	85	90	329	1.375	6.88
C8	Internal heating network	Water	Liquid	51.4	73.2	29.5	0.123	2.69
C9	Steam demand: Drying section	-	-	138.7	-	-	-	43.30
C10	Steam demand: Degassing	-	-	133.6	-	-	-	40.23
C11	Steam demand: Cooking liquor	-	-	176	-	-	-	26.06
C12	Steam demand: O_2-reactor	-	-	176	-	-	-	3.42
C13	Steam demand: Bleaching	-	-	133.6	-	-	-	1.17
C14	Steam demand: PO/OP-stage	-	-	194.3	-	-	-	9.76
C15	Steam demand: Evaporation, LP	-	-	133.6	-	-	-	81.89
C16	Steam demand: Evaporation, MP	-	-	176	-	-	-	14.29
C17	Steam demand: Chemical preparation	-	-	133.6	-	-	-	1.04

65.6 °C. This can be seen in Figure 5.2 where the area inside the circle represents a near-pinch. However, for ΔT_{min} lower than 10 °C, the pinch is robust and only increases to 112.4 °C for a ΔT_{min} of 1 °C. The current use of ΔT_{min} of 10 °C is considered to be on the safe side as several heat exchangers in the mill with lower ΔT_{min} exist. An example of this would be the heat exchange between bleaching backwater and the water in the sawmill heating network.

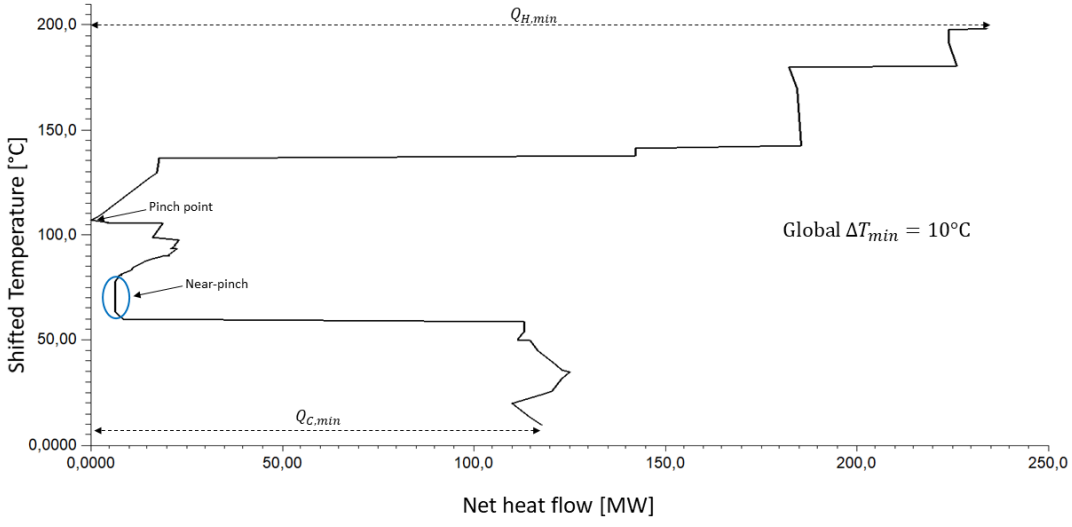

Figure 5.2: The Grand Composite Curve obtained from the hot and cold stream Tables 5.1 & 5.2.

The minimum heating demand, $Q_{H,min}$, and cooling demand, $Q_{C,min}$, for given data extraction is graphically visualised in the GCC in Figure 5.2. The actual and minimum heating demand values are also presented in Table 5.3. The targeting value of $Q_{H,min}$ is determined by Aspen Energy Analyzer and the actual heating demand can be obtained by summarising all the steam consumers in the cold stream Table 5.2. Cold streams C9-C17 represent aggregated steam demands for process areas which are insufficiently mapped. The temperatures are set equal to the condensation temperature for given pressure level and shifted with ΔT_{min}. The steam consumers are mostly found in C9-C17 but 40.5 MW of the actual steam demand seen in Table 5.3 are also found in C1, C2, C4 & C7. The potential savings of 27.7 MW, corresponding to the difference $Q_{H,actual}$-$Q_{H,min}$, could theoretically be achieved by eliminating pinch violations. However, the highest tank temperature in the SHS is 85 °C which mean that a gap exist between the cold pinch and the HW-tank temperature. Thus, in order to remove the pinch violations either process to process heat exchange is needed or one can create a temperature level in the SHS which is higher than 85 °C.

Table 5.3: The minimum heating demand from the energy targeting in Aspen Energy Analyzer and the actual heating demand aggregated from Table 5.2.

Heating	MW
$Q_{H,min}$	234
$Q_{H,actual}$	261.7

5.5 Description of operating cases

The stream data presented in Section 5.4 is an updated list of the work of Nihlmark and Mahmoud [7]. This data set stems from spring conditions. Data was extracted between 2017-03-10 to 2017-03-27 on an hourly resolution, and the used data set is the average values of the extracted data. This period is considered as the spring case and will be the starting point for the different retrofits. Normally during retrofits a data set is extracted that is supposed to represent the whole year. However, if analysing data over a larger time span it can be seen that supply temperatures are affected by outdoor conditions and e.g. the supply demand of heating networks change [16]. The MATLAB-tool makes it possible to take this into account and easily change between different operating conditions and thereby quantify the actual steam savings with a higher time resolution.

To give a good representation of the network performance three different time spans are picked based on the seasons of the year. The spring conditions are in this case considered to be similar as for autumn. Autumn is therefore not specifically evaluated and is assumed to be identical to spring. The assumption is reasonable because the mean outdoor temperature according to SMHI during 2017 was 4 °C in March and 4.2 °C in November in Kalmar [22]. To give a good representation, additional data for the spring case was extracted in Södras process monitoring system and the same filtering process is used as in the work of Nihlmark and Mahmoud. An overview of the filtering criteria can be seen in Table 5.4. The first filtering cri-

teria regards that the mill produces softwood pulp during all the extracted hours to give a consistent representation. The second criteria make sure that the data sets were picked during periods of high production. High and stable production were defined as, in collaboration with mill engineers at Södra, when the recovery boiler is operating at $\geq$ 98 % of its design capacity. The filtering of outdoor air- and water temperatures represent the conditions at the mill during which manual measurements were performed by Nihlmark and Mahmoud.

The two other operational data sets are for summer and winter conditions. The data set for summer was extracted for the operating period 2017-06-02 to 2017-06-22. During this period the mean outdoor temperature in Kalmar was 15.6 °C according to SMHI's statistics [22]. It was not the warmest summer month but when comparing hours of high production, seen as column 2 in Table 5.4, it was the most consistent compared to July and August. The share of measurement hours that made it through the filtering criteria seen in Table 5.4 was 75.6 % for June and 36.3 % and 43.8 % respectively for July and August.

For winter conditions the data set was extracted for the operating period 2018-02-07 to 2018-02-23. During this period the mean outdoor temperature in Kalmar was -2.4 °C [22]. That month had the coldest mean temperature during the period 2016-11-01 to 2018-03-14. It was also very consistent in terms of production as the capacity of the recovery boiler was above 98 % of the design capacity during the whole time span. The extracted data for summer and winter were only filtered regarding softwood pulp production and the operating capacity of the recovery boiler. No temperature filtering was performed as no manual on-site measurements were performed for this period of time.

Table 5.4: An overview of the filtering criteria for the three different time spans.

	Softwood pulp production	RB operated at $\geq$ 98 % of design capacity	Temperature Emån 2-6 °C	-5 $\leq$ T $\leq$ 8 of wood yard & sawmill
Spring	✓	✓	✓	✓
Summer	✓	✓	-	-
Winter	✓	✓	-	-

6
Case Study - Retrofit

This chapter presents and analyses two retrofit proposals derived during the case study. The retrofits are derived based on the stream data for springtime operation described in Section 5.4. Both retrofit proposals are further analysed for winter and summer operation. For the second retrofit proposal, the developed MATLAB-tool is used to evaluate the effect of changing conditions and to optimise operational settings for each investigated season. An overview of the retrofit designs and the performed analyses are given in Section 6.1, and more detailed descriptions are given in Sections 6.2-6.4. The results obtained by the MATLAB-tool are validated in Section 6.5 by comparing it to a more advanced heat exchanger model obtained from Södra.

6.1 Overview of retrofit designs

There are two main retrofits; Retrofit 1 and 2. Retrofit 1, described in Section 6.2, aims at generating a water stream with a temperature above 100 °C in the secondary heating system. Below, this water stream is referred to as Very Hot Water (VHW). The VHW allows heating cold streams closer to the cold pinch point, and Retrofit 2, described in Section 6.3, aims at utilising the VHW to replace steam for heating of feed water and combustion air. Consequently, the two retrofits are dependent on each other.

6.1.1 Retrofit 1

Retrofit 1 is a redesign of the mill's digester section. Retrofit 1 is not analysed using the developed MATLAB-tool. However, this retrofit generates a very hot water stream which is used as a supply stream in Retrofit 2, which is analysed using the MATLAB-tool. The temperature and flowrate of the VHW varies between seasons. To be able to perform the analysis of Retrofit 2, the temperature and flowrate of the VHW stream generated in Retrofit 1 is calculated for all seasons, as described in Section 6.2.

6.1.2 Retrofit 2

Retrofit 2 is a redesign of the mill's mist condenser circuit, and utilises the VHW generated in Retrofit 1 to replace steam for heating of feed water and combustion

air. For Retrofit 2, there are four different design cases and one base case. The base case, described in Section 6.3.2, installs two new heat exchangers and increases the size of one existing. The required UA-values are calculated using springtime operating conditions and the operational settings which are currently used at the mill for these operating conditions.

The base case is developed into four different design cases (D1-D4), described in Section 6.4.1. The design cases include slight variations in network structure compared to the base case, but the exchanger sizes are the same. Since capital costs are not taken into account in this work, using the same exchanger sizes facilitates an economic comparison of the designs.

The four design cases are analysed for spring, winter and summer operating conditions using the developed MATLAB-tool. For each investigated condition, operational settings are optimised using the MATLAB-tool to give a fair comparison between the designs. For summer and winter operating conditions, comparisons are made between using the operational settings which were optimised for spring and using settings optimised for the relevant seasons. This illustrates the importance of adjusting operational settings when evaluating the performance of a design. The results of these analyses are given in Section 6.4.2.

Note that the base case is not analysed using the MATLAB-tool. Beyond serving as a dimensioning case for new or extended units in the four design cases, the base case gives an idea of what steam savings would be achieved without using the MATLAB-tool. Without an easy, straightforward way of solving network temperatures for changing network parameters, the operational settings in the studied system would likely be maintained. Additionally, the retrofit would likely be performed on a smaller system boundary, which constrains the design options. This is illustrated when the base case for Retrofit 2 is derived in Section 6.3.

6.2 Retrofit 1 - Digester section

There are several hot process streams in the digester section with temperatures above 100 °C. These streams are cooled using warm water which is thereby heated to temperatures at or above the hot water level of 85 °C. Thus, the digester section can be said to produce hot water. The aim of this retrofit is to produce very hot water (VHW), at temperatures above 100 °C, in the digester section. The data required for a complete analysis of this retrofit is only available for springtime operating conditions. However, in the end of this section, estimates are used to analyse performance for winter and summer conditions as well. The retrofit will affect both the heat and the mass balance of the HW-tank. This is discussed further in Section 6.2.1.

Currently, most heat exchangers in the digester section are operated in parallel; warm water is heated and sent to the hot water tank. By retrofitting parts of the digester section and placing heat exchangers in series instead of in parallel, a smaller

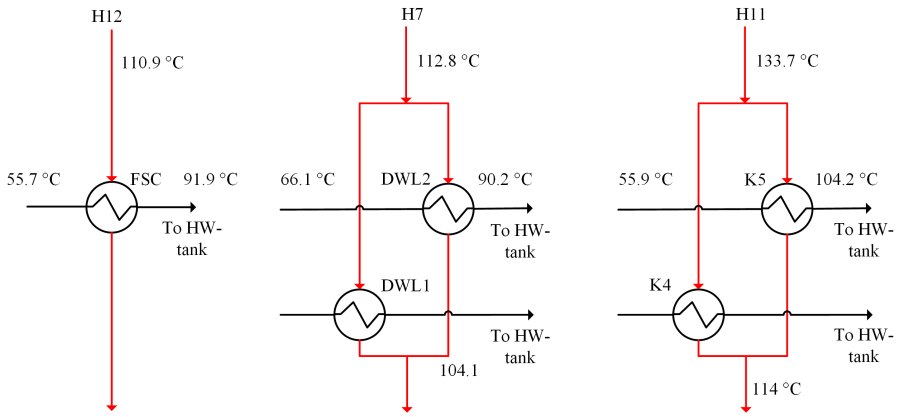

Figure 6.1: Current layout of the retrofitted part of the digester section. FSC, DWL2 and K5 are affected by the retrofit. Black: SHS, Red: Hot process streams. All HW is sent directly to the HW-tank.

amount of VHW can be produced instead of a larger amount of HW. The generated VHW can be used to heat cold process streams to temperatures above the hot water tank temperature of 85 °C, which is the current limit to indirect heat exchange via the secondary heating system. Doing this, the high temperatures of the hot process streams in the digester section can be better utilised. It should also be noted that the digester section is considered as a stable supplier, whenever the mill is operating, so is the digester section.

In the retrofitted digester section, hot streams H7, H11 and H12 are used to produce VHW. H7 is currently cooled in four different exchangers and one of these, DWL2, is adjusted in the retrofit. H11 is cooled in two exchangers and one of them, K5, is adjusted in the retrofit. H12 is a condensing stream, cooled in two exchangers of which one, FSC, is adjusted in the retrofit. The exchangers that are not adjusted operate at exactly the same conditions before and after the retrofit. Currently, DWL2, FSC and K5 all operate in parallel with respect to the water side of the exchangers and produce HW directly to the HW-tank. This is visualised in Figure 6.1. Current operating and design data for the three exchangers is tabulated in Table 6.1. The listed UA-values are calculated from the given temperatures and duties.

Table 6.1: Current operating and design data for heat exchangers affected by the digester section retrofit.

Unit	Duty [kW]	Water flow-rate [l/s]	$T_{H,in}$ [°C]	$T_{H,out}$ [°C]	$T_{C,in}$ [°C]	$T_{C,out}$ [°C]	ΔT_{lm} [°C]	UA [kW/K]
FSC	6687	44.2	110.9	110.9	55.7	91.9	33.9	197.0
DWL2	7771	77.2	112.8	104.1	66.1	90.2	29.7	262.0
K5	2019	10	133.7	114	55.9	104.2	42.2	47.8

In the retrofit, warm water is sent first to FSC and then to DWL2 and K5, in that order. The total water flow is made up of the 77.2 l/s currently entering DWL2, mixed with 4.6 l/s of the water currently entering FSC. This gives a total flowrate

of 81.8 l/s and a starting temperature of 65.5 °C. The additional 4.6 l/s allows minimum temperature differences in the retrofitted digester section to be at least 5 °C.

Since the main task of DWL2, FSC and K5 is not to produce HW (or VHW) in the secondary heating system but to cool process streams by a certain amount, their duties must be the same after the retrofit. Since they will be put in series to produce hotter water, temperature driving forces will go down and UA-values must be increased. Table 6.2 lists heat exchanger temperatures and UA-values after the retrofit. With maintained duties for the exchangers and a starting temperature of 65.5 °C, 81.8 l/s of VHW at 113.7 °C can be produced in the retrofit. Below, the final VHW temperature is referred to as the VHW supply temperature.

Table 6.2: New operating and design data for heat exchangers affected by the digester section retrofit.

Unit	Duty [kW]	Water flow-rate [l/s]	$T_{H,in}$ [°C]	$T_{H,out}$ [°C]	$T_{C,in}$ [°C]	$T_{C,out}$ [°C]	ΔT_{lm} [°C]	UA [kW/K]
FSC	6687	81.8	110.9	110.9	65.5	85.1	34.7	192.8
DWL2	7771	81.8	112.8	104.1	85.1	107.8	10.5	740.3
K5	2019	81.8	133.7	114	107.8	113.7	11.8	171.3

The drawback of placing the heat exchangers in series is, besides the need for increased UA-values, that the mass and energy balances for the hot water tank are affected. This effect, and remedying options, are described in more detail in Section 6.2.1. The retrofitted digester section is visualised in Figure 6.2 where it can be seen that the three heat exchangers now are in series.

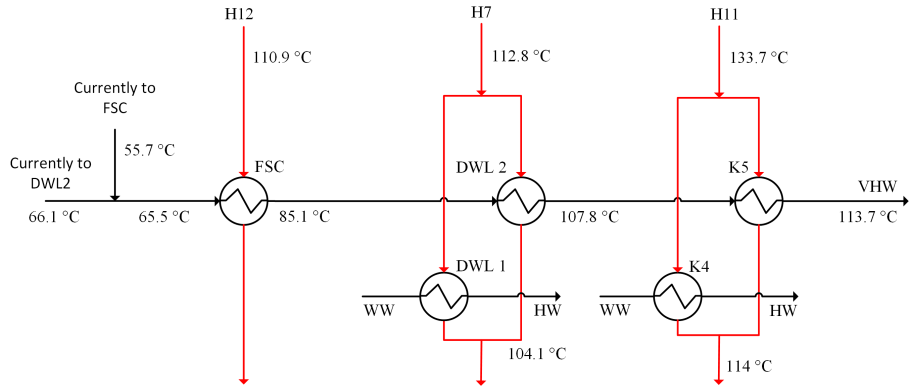

Figure 6.2: Retrofit for VHW generation in the digester section. Black: SHS, Red: Hot process streams.

The analysis above is valid for the springtime operating conditions established by Nihlmark and Mahmoud [7]. The mill digester section is poorly mapped and the retrofit proposal described above and illustrated in Figure 6.2 is to some extent based on on-site measurements done by Nihlmark and Mahmoud. Such measurements are

not available for winter or summer operation and additionally, the availability of heat exchanger data is low. Because of this, the digester section retrofit is not analysed using the MATLAB-tool. This decision is further motivated by the limited size and low complexity of the retrofit, making it unlikely that any significant improvements would be identified using the tool. However, the VHW-stream generated in this retrofit is a crucial input in Retrofit 2. Therefore, the supply temperature and flowrate of VHW that can be generated in the digester section must be estimated for winter and summer conditions as well. To achieve this, the duty of the three exchangers FSC, DWL2 and K5 used in the retrofit must be known or estimated. The starting point for VHW generation in the retrofit is achieved by mixing of WW-flows currently entering exchangers DWL2 and FSC (see Figure 6.2) meaning that these parameters must be known as well.

For winter and summer conditions, available data is enough to calculate the duty of heat exchanger FSC, but data for DWL2 and K5 is lacking. The unknown duties are assumed constant for all seasons. For DWL2, this assumption is supported by the fact that the dilute liquor flow to the two parallel exchangers DWL1 and DWL2 is not changing between seasons, and that the target temperature of this stream is a hard target. For K5, the duty given by Nihlmark and Mahmoud is considered conservative since measurements made by process engineers indicate that significantly higher duties are common.

If the duty of DWL2 is assumed constant, the inlet temperature on the secondary heating side can be calculated. The corresponding inlet to FSC is measured by process monitoring systems, meaning the retrofit inlet to FSC (see Figure 6.2) can be calculated for a given mixing ratio.

Table 6.3: Estimated flowrate and supply temperature of very hot water (VHW) generated in the digester section, for spring, winter and summer operating conditions.

	VHW flowrate [l/s]	Q_{FSC} [MW]	$T_{in,FSC}$ [°C]	$T_{in,DWL2}$ [°C]	$T_{in,K5}$ [°C]	$T_{VHW,Supply}$ [°C]
Spring	81.8	6.9	65.5	85.1	107.8	113.7
Winter	88.7	10.8	55.1	86.8	107.8	113.2
Summer	81.8	4.9	60.6	75.0	97.7	103.6

For a given flowrate and with the assumptions made above, the VHW supply temperature can be calculated through a heat balance. Table 6.3 lists the flowrate and supply temperature of the VHW generated in the digester section for the three investigated seasons. The duty of FSC, which varies between seasons, is also listed. For summer operation, the flowrate of the VHW was maintained at the spring value. For winter operation, the high duty of exchanger FSC risks causing driving force problems in exchanger DWL2. Therefore, the VHW flowrate is increased to keep the outlet temperature from DWL2 at the springtime value of 107.8 °C.

6.2.1 Hot water balance

The retrofit of the digester section described in Section 6.2 leads to a loss of hot water that affects the quantity of water sent to the hot water tank, as well as the temperature of that water. The measures taken to restore the mass balance are described below, using data for springtime operating conditions. At the end of this section, the results of similar analyses for winter and summer conditions are listed.

The third column of Table 6.1 gives the amount of hot water currently sent to the hot water tank from the three exchangers FSC, DWL2 and K5 during springtime operation. The corresponding temperatures are listed in the seventh column. Using this data, the flow of hot water to the tank can be calculated to 131.4 l/s at an average temperature of 91.8 °C. In order to maintain the mass and energy balance of the tank after the retrofit, both temperature and flowrate of the water sent to the tank must be maintained.

Regarding the mass balance, the 81.8 l/s of VHW generated in the digester section retrofit will be sent to the hot water tank after use in Retrofit 2, as described in Section 6.3. Consequently, the remaining loss is 131.4-81.8=49.6 l/s. This loss of HW can partly be compensated by a minor retrofit involving the MCO2 exchanger. In this exchanger, hot stream H3 is cooled from 94 °C to 84.4 °C before being used in the oxygen bleaching process. The secondary heating system is used for cooling; the cold inlet is directly from the CW-tank and the outlet is sent directly to the WW-tank. If H3 is instead cooled by water directly from the WW-tank, 36.7 l/s of HW can be produced and sent to the HW-tank. Since nothing is changed on the process side of the exchanger, and the secondary heating system side is directly connected to two tanks both before and after the retrofit, no impact on the overall process is expected due to this retrofit. The only exception is the mass balance for the WW-tank. Using the MCO2 exchanger to produce HW means a double loss of WW; the current production in the MCO2 exchanger is lost and WW is instead used to produce HW. However, the mill currently has a large overflow of WW and there is an additional amount of 49.6 l/s of WW due to the retrofit itself (see above). Consequently, this means that no shortage in WW is expected.

Generating HW in the MCO2 exchanger means lower temperature driving forces, and an increase in exchanger size is required. Table 6.4 compares operational settings and design parameters for the MCO2 exchanger before and after the retrofit.

Table 6.4: Operating and design data for the MCO2 exchanger before and after being retrofitted for HW production.

Unit	Duty [kW]	Water flow-rate [l/s]	$T_{H,in}$ [°C]	$T_{H,out}$ [°C]	$T_{C,in}$ [°C]	$T_{C,out}$ [°C]	ΔT_{lm} [°C]	UA [kW/K]
MCO2 (old)	4600	32.9	94	84.4	16.8	50.2	54.8	83.9
MCO2 (new)	4600	36.7	94	84.4	55	85	17.2	266.9

The retrofit of the digester section for VHW production is considered to always in-

clude HW production in the MCO2 exchanger. The remaining loss of HW resulting from the digester retrofit is 49.6-36.7=12.9 l/s. The remaining loss of hot water is initially assumed to be covered by steam heating of warm water to hot water. The required steam consumption is 1.6 MW. However, when Retrofit 2 is analysed further in Section 6.4 it will be demonstrated that these 12.9 l/s can be brought to the hot water temperature without using steam.

As mentioned above, the average temperature of the 131.4 l/s sent to the hot water tank must be 91.8 °C to maintain the heat balance. This limits the temperature of the VHW sent to the HW-tank after use in Retrofit 2, hereafter referred to as the VHW return temperature. With 49.6 l/s sent to the hot water tank at 85 °C, the remaining 81.8 l/s of VHW from the digester section must not be below 95.9 °C if the average temperature of 91.8 °C is to be maintained.

The analysis above is for springtime operating conditions. However, both the flowrate and the temperature of the hot water sent to the HW-tank from heat exchangers FSC, DWL2 and K5 before the retrofit are available for all seasons. The duty of MCO2 can be calculated for all seasons, meaning the amount of hot water produced in this exchanger can also be calculated. Consequently, the analysis can be repeated for all seasons using the VHW flowrates listed in Table 6.3. The resulting lower bound for the VHW return temperature is listed for all seasons in Table 6.5.

Flowrates and temperatures of the hot water streams sent to the HW-tank after the retrofit are summarised in Table 6.5. For hot water sent to the HW-tank before the retrofit, the corresponding information is available for springtime operating conditions in Table 6.1.

Table 6.5: An overview of the flowrates and temperatures used for the heat balance of the HW-tank before and after the retrofit.

	Before retrofit		After retrofit					
	FSC+DWL2+K5		MCO2		Steam heating of make-up WW		VHW return	
	Flowrate [l/s]	Temp. [°C]	Flowrate [l/s]	Temp. [°C]	Flowrate [l/s]	Temp. [°C]	Flowrate [l/s]	Temp. [°C]
Spring	131.4	91.8	36.7	85	12.9	85	81.8	≥95.9
Winter	136.5	91.8	26.6	85	21.2	85	88.7	≥95.5
Summer	133.1	86.4	37.7	85	13.6	85	81.8	≥87.3

6.3 Retrofit 2 - Base case

The focus of Retrofit 2 is the mist condenser circuit at Södra Cell Mönsterås. The mist condenser circuit includes two large steam heaters used for preheating of combustion air and feed water. In this section the current situation in the mill is presented along with a base case retrofit. The retrofit solution makes use of the VHW

produced in the digester section to replace steam for air and feed water heating. The base case retrofit is derived using the springtime stream data described in Section 5.4. Additionally, all operational settings (split ratios, bypass ratios) in the mist condenser circuit are maintained to reflect the current operation. In Section 6.4, the base case is developed into four additional designs which are analysed for variations in operating conditions and operational settings using the MATLAB-tool.

6.3.1 Current situation

This section describes the current operating conditions for Södra Cell Mönsterås' mist condenser circuit, which is visualised in Figure 6.3 and which is the focus of Retrofit 2. When smelt discharge from the recovery boiler is mixed with weak liquor to produce green liquor, intense reactions produce water vapour which mixes with surrounding air to give a mist (moist air). This mist is represented by stream H5 in Table 5.1 and is condensed in the mist condenser (MC in Figure 6.3) using water from the secondary heating system as cooling media. Condensation of the mist is not a process requirement, and the amount that is not condensed is vented to the atmosphere. The mist condenser is currently set to produce hot water at 86.2 °C. Significantly higher temperatures cannot be achieved, since the start temperature of H5 is 90 °C.

The HW that is produced in the mist condenser delivers heat to four cold streams. These are feed water to the bark and recovery boilers (C1/C2 in Table 5.2), combustion air to the recovery boiler (C3) and the mill's internal heating network (C8) which in turn heats the mill premises. The mist condenser circuit includes three different steam heaters. Two major ones are represented by preheating of air and feed water along with a smaller one on the internal heating circuit.

The supply and target temperatures for the boiler air are around 30 °C and 165 °C respectively, depending on season. Currently, preheating is done, first by air-batteries that make use of hot water, and then by steam heaters. The hot water is in a closed circuit seperated from the SHS for safety reasons so a potential leakage of water into the boiler can be controlled and stopped. The water in the closed circuit is heated in VVX7 by hot water produced in the mist condenser. The hot water circuit heats the combustion air to 64.6 °C and the remaining heating, to 165 °C, is done using steam. The current limitation of the heating in the air batteries is the temperature of the hot water in the closed circuit. Thus, increasing this temperature makes it possible to preheat the air further and save steam.

The feed water (C1/C2) starts at roughly 8 or 30 °C and is heated to 125 °C. Currently, 53.9 l/s of the total feedwater flow is heated in exchangers VVX11A/B which are included in the mist condenser circuit. However, before being supplied to VVX11A/B these 53.9 l/s are heated outside the system boundary of the mist condenser and the supply of feed water to VVX11A/B is 82.5 °C. The feed water is heated by VVX11A/B and afterwards heated by steam from 84.6 °C. The steam heating mainly occurs in the feed water tanks. Here, the feed water need some

steam for degassing but the preheating to the saturated temperature of 125 °C can be done by another heat source.

The water in the internal heating network (C8) is heated in VVX2:1 and VVX2:2 by the hot water produced by the mist condenser. During spring conditions, this is enough to reach the target temperature of 73 °C and no steam heating is used.

The pinch violations in the mist condenser circuit are in the form of (steam) heating of air and feed water below the pinch. The violations are listed in Table 6.6.

Table 6.6: Current pinch violations in the mist condenser circuit.

Location	Type	Amount [MW]
Feed water	Heating below	4.1
Combustion air	Heating below	6.0

6.3.2 Retrofit

The goal of Retrofit 2 is to reduce the total steam consumption in the mill's mist condenser circuit, by making use of the VHW produced in Retrofit 1. This VHW is used for preheating of air and feed water. A new heat exchanger is installed in the closed hot water circuit to increase the temperature of water into the air batteries and thereby save steam. To make full use of the increased temperature of the hot water, the size (UA-value) of the air battery is increased. The VHW is also used in a new heat exchanger to preheat the feed water even further before steam is used. For the base case retrofit (i.e. not using the MATLAB-tool) described in this section, all calculations are done by hand. As previously mentioned, springtime operating data is used and current operational settings are maintained. The UA-values are calculated for true counter-current heat exchangers from existing temperature and flow measurements. Due to iterative calculations it is difficult and time consuming to analyse the entire network of Figure 6.3. The system boundary for this retrofit is instead decreased and the new system boundary is seen in Figure 6.4.

The studied system now consists only of the closed water circuit, the combustion air, the feed water stream and the VHW stream from the digester section. To make sure that nothing outside the system boundary is affected by the retrofit, the temperature of the closed water circuit to VVX7 must be maintained in the retrofit. This means that the size of the new heat exchanger (New1) installed on the closed water circuit must be accompanied by an increase in air battery size to keep the inlet temperature to VVX7 the same. No similar precautions are necessary for the new feed water exchanger (New2); the two outlet streams are directed to tanks and will not impact temperatures in the surrounding system.

The new exchanger New1 is designed to operate with a minimum approach temperature difference of 5K. Heat exchanger New2 is constrained by the requirement to maintain the heat balance for the hot water tank. As described in Section 6.2.1,

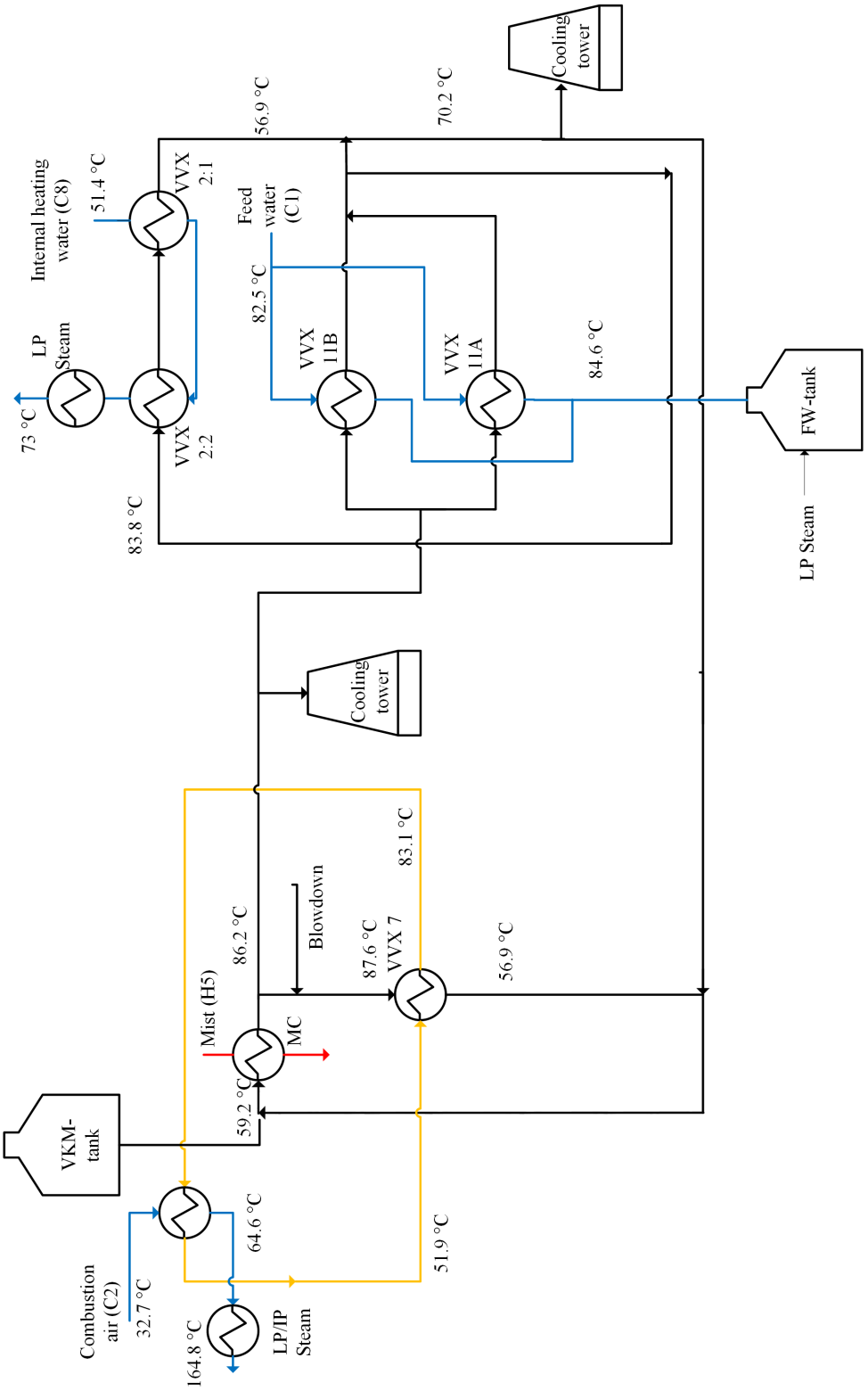

Figure 6.3: The mist condenser circuit at Södra Cell Mönsterås. The given temperatures are for springtime operation. Black: SHS, Orange: closed water circuit, Blue: cold process stream, Red: hot process stream.

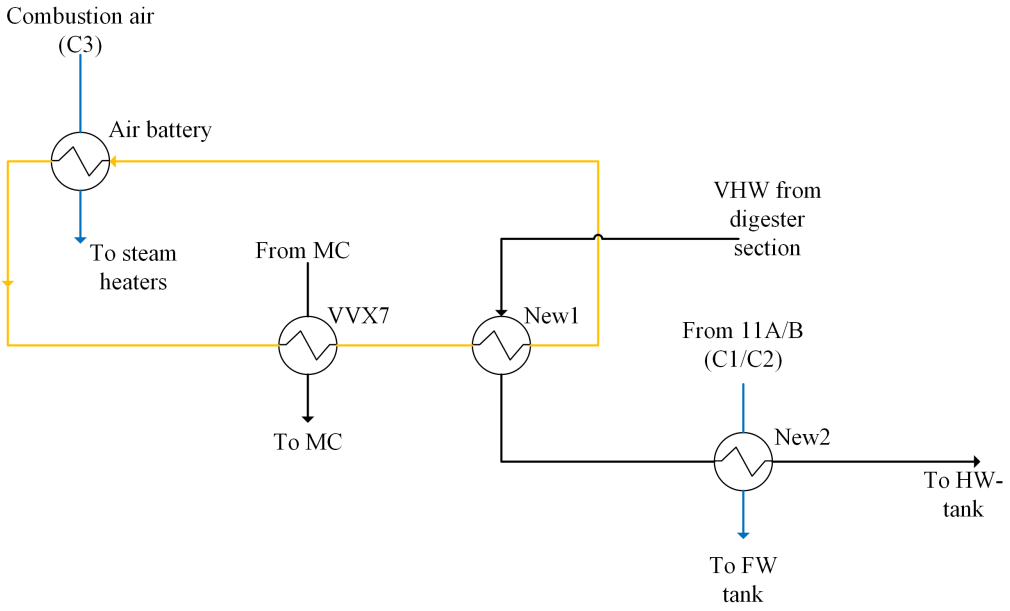

Figure 6.4: The base case retrofit of the mist condenser circuit. The VHW stream generated in Retrofit 1 is heat exchanged in the two new exchangers New1 and New2. The size of the air battery is increased. Black: SHS, Orange: closed water circuit, Blue: cold process stream.

this requires the VHW outlet temperature to be at least 95.9 °C. The air battery UA-value is increased to keep the warm water inlet temperature to VVX7 the same as in the base case. Resulting operating and design data for new and modified exchangers are given in Table 6.7.

Table 6.7: Operating and design data for heat exchangers installed, or modified, in the mist condenser circuit retrofit.

Unit	Duty [kW]	$T_{H,in}$ [°C]	$T_{H,out}$ [°C]	$T_{C,in}$ [°C]	$T_{C,out}$ [°C]	ΔT_{lm} [°C]	UA [kW/K]
New1	4077	113.7	101.8	83.1	108.7	10.4	392.8
New2	2004	101.8	95.9	84.7	96.8	9.7	207.1
Air battery (new)	9043	108.7	51.9	32.7	90.8	18.5	487.8
Air battery (old)	4966	83.1	51.9	32.7	64.6	18.8	263.5

This achieves steam savings of 4.1 MW for air pre-heating and 2.0 MW for feed water heating, totalling 6.1 MW. Since neither the feed water nor the combustion air reach the cold pinch temperature, the pinch violations in Table 6.6 are reduced by the same amount. The solution presented above does not regenerate any of the hot water lost in the digester section retrofit. This means that 12.9 l/s of hot water must be generated elsewhere. As was described in Section 6.2.1, this loss is initially assumed to be covered by steam heating from the warm water to the hot water temperature. This gives a steam penalty of 1.6 MW, which can be considered heating

below the pinch, reducing the steam savings to 4.5 MW.

Note that the heat used in the retrofit derives from the hot process streams in the digester section that were used to generate VHW in Retrofit 1. Consequently, Retrofits 1 and 2 imply indirect heat exchange between hot streams in the digester section and the cold air and feed water streams. Since the hot process stream entering K5 is above the hot pinch temperature (Section 6.2), this solution includes cross-pinch heat transfer. The process stream in K5 has a target temperature above the hot pinch temperature, meaning the 2 MW heat transfer in K5 is entirely through the pinch. However, this process stream was already heat exchanged via the secondary heating before the retrofit, meaning that the pinch violation is not introduced by the retrofit. The same reasoning holds for the first 0.3 °C of cooling of the hot process stream in DWL2, which starts at 112.8 °C. This 0.3 °C cooling constitutes a 0.3 MW cross-pinch heat transfer.

Pinch violations before and after the combined retrofits of the digester section and the mist condenser circuit are summarised in Table 6.8.

Table 6.8: Pinch violations in the digester section and the mist condenser circuit, before and after Retrofits 1 and 2.

Description	Type	Before retrofit [MW]	After retrofit [MW]
Feed water heating	Heating below pinch	4.1	2.1
Air pre-heating	Heating below pinch	6.0	1.9
Heating of warm water	Heating below pinch	-	1.6
Exchanger K5	Cross-pinch heat transfer	2.3	2.3
Total pinch violations		12.4	7.9
Savings			4.5

6.4 Retrofit 2 - Analysis of design cases

This section involves a further analysis of the base case retrofit presented in Section 6.3.2. The base case retrofit is developed to four different designs which are analysed with the help of the MATLAB-tool in Section 6.4.2. The general approach for developing the new retrofit proposals is to use a common foundation. All the retrofits use the design data of the heat exchangers, seen in Table 6.7, derived from the base

case retrofit that was developed for spring conditions. The different designs are then analysed for spring, winter and summer while trying to maximise the steam savings.

6.4.1 Description of design cases

The base case retrofit of the mist condenser circuit during spring conditions is described in Section 6.3 and is combined with the digester section retrofit described in Section 6.2. During all seasons, this solution is associated with HW losses according to the analyses in Section 6.2.1. As illustrated in Figure 6.3, HW from the mist condenser circuit is currently bled to a cooling tower. This HW can instead be sent to the HW-tank to make up for some of the loss in the digester retrofit.

The detailed analysis of the mist condenser circuit aims at increasing the HW flow to restore the mass balance for the HW-tank, while increasing the steam savings. The analysis is performed using the MATLAB-tool and the system boundary is increased to include the entire circuit of Figure 6.3.

The analysis starts by improving the base case retrofit of the mist condenser circuit, described in Section 6.3 and seen in Figure 6.4. This is done by sending HW to the tank instead of the cooling tower. The resulting design is seen as Design 1 in Table 6.9. Design 1 is also visualised in Figure 6.5. The only difference compared to the base case design is that no water is sent to cooling towers and that hot water is instead extracted to the HW-tank. Three additional different design variations are then investigated. These regard the sequencing of the VHW and whether VVX11A&B in Figure 6.5 should connect with the VHW from the digester section or with the HW from the mist condenser. In the latter, a new additional heat exchanger is installed to heat the feed water with the VHW which is similar as in the base case. All four designs send HW to the HW-tank instead of the cooling tower, and make use of the VHW from the digester retrofit, the increased area of air batteries and heat exchanger New1 introduced in Section 6.3 for the base case retrofit. An overview of the different designs is seen in Table 6.9 and flow charts are found in Appendix C.

Operational settings in the four designs are first optimised for spring conditions and the performance is evaluated. The performance of the four heat exchanger networks is then analysed under two new sets of operating conditions: winter and summer. The flexibility of the network is used to adapt to the changing conditions, with the goal of increasing steam savings compared to using operational settings which are optimised for spring, and recover all lost HW. Additional design changes which enhance the network's ability to adapt to changing conditions are also evaluated if needed.

Table 6.9: An overview of the four different designs investigated for the different seasons.

	Keep VVX 11AB	Move VVX 11AB	Air -> FW	FW -> Air
Design 1	✓		✓	
Design 2	✓			✓
Design 3		✓		✓
Design 4		✓	✓	

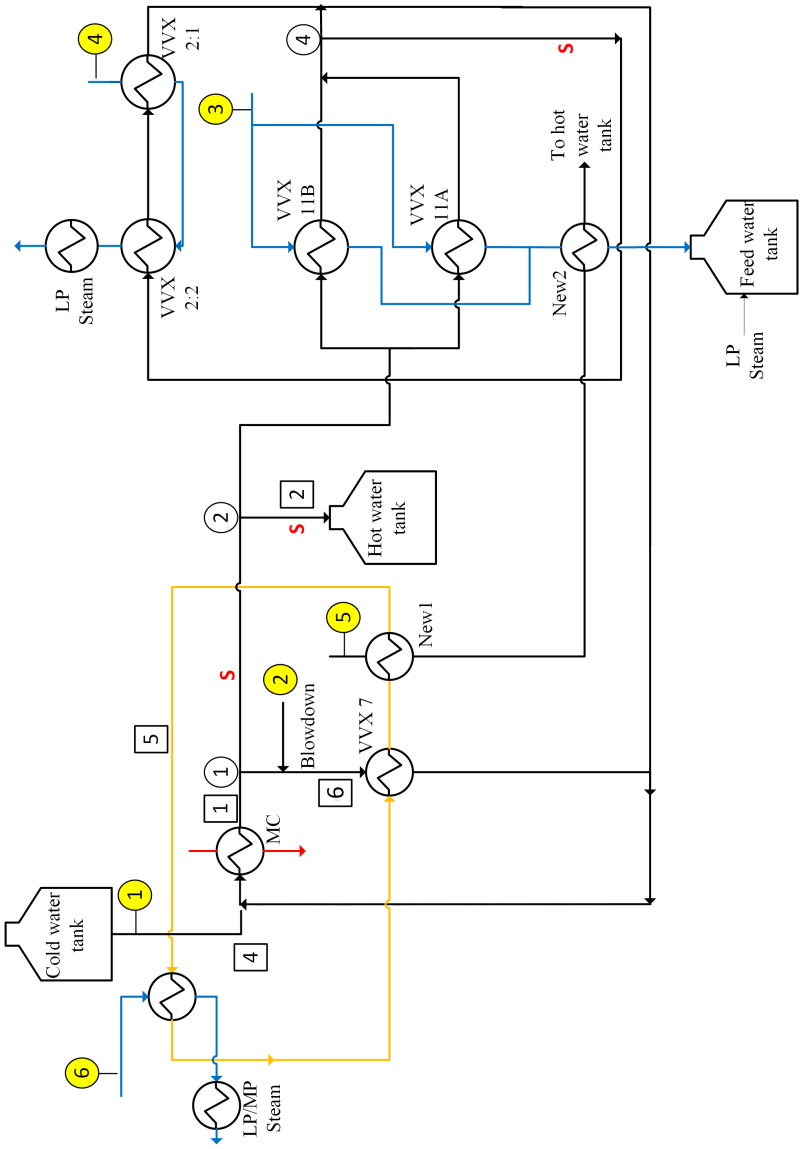

Figure 6.5: Retrofit design D1 of the mist condenser circuit. *Yellow circle:* input data point, from Table 6.10. *White circle:* Split number, from Tables 6.12, 6.13 and 6.14. Split ratio definition: (Flowrate of outlet stream marked S)/(Flowrate of inlet stream). *White square:* Stream number, from Tables 6.12, 6.13 and 6.14.

Operating conditions and constraints

As described in Section 6.4.1 the four different designs are evaluated under different operating conditions; spring, winter and summer. The heat exchangers are already dimensioned from the base case in Section 6.3 and these UA-values are updated using the correction factor. This implies that only supply temperatures and flowrates are needed for the summer and winter operational cases for the MATLAB-tool to calculate all energy and mass balances in the heat exchanger networks. The temperatures and flowrates of the supply streams for the different operating conditions is presented in Table 6.10. It should be noted that the flowrate coming from the CW-tank is adjustable and therefore no specific value is presented. The use of the CW-flow is described further in Section 6.4.2.

Table 6.10: The supply conditions given to the MATLAB-tool for the mist condenser circuit for every season. Supply stream number refer to yellow circles in Figure 6.5.

Supply stream number	Description	Spring	Summer	Winter
1	Temperature CW-tank [°C]	16.8	19.4	12.3
	Flowrate from CW-tank [kg/s]	-	-	-
2	Temperature blowdown [°C]	92.5	93.6	92.1
	Flowrate blowdown [kg/s]	8.9	9.5	9.4
3	Feed water temperature to VVX 11A&B [°C]	82.5	86.6	80.3
	Feed water flowrate to VVX 11A&B [kg/s]	53.9	47.5	62.0
4	Temperature internal heating network [°C]	51.4	62.9	49.4
	Flow internal heating network [kg/s]	29.5	28.7	32.2
5	Temperature of very hot water [°C]	113.7	103.6	113.2
	Flowrate of very hot water [kg/s]	81.8	81.8	88.7
6	Temperature of air to boiler [°C]	32.7	36.9	31.4
	Flowrate of air to boiler [kg/s]	154.9	153.4	156.9

During the investigation of different design cases for the mist condenser circuit, several constraints are imposed on the system. These are limits on allowed flowrates and heat extraction. The two available heat sources are the mist condenser itself and the VHW stream generated in the digester section retrofit, which is described in Section 6.2.

The mist condenser exchanger makes use of waste mist from the recovery boiler and the goal is to utilise it as much as possible. The process side target temperature is soft and the mist condenser is flexible in the sense that a specified target temperature on the secondary heating system side can be reached under a wide range of flowrates and inlet temperatures. For this reason, the mist condenser is modelled as a utility exchanger with fixed target temperature. After consultation with mill engineers, the duty of the mist condenser was limited to 15 MW. The constraints of the mist condenser during operation for the different seasons are seen in Table 6.11.

The hot water sent to the HW-tank (Stream 2 in Figure 6.5) will be at the same temperature as the mist condenser outlet. This temperature is listed in column 2 of Table 6.11. As mentioned in Section 6.4.1, the HW-extraction is for all design cases and operating conditions taken to be enough to restore the HW-tank mass balance to compensate the deficit described in Section 6.2.1. The HW extracted

from the mist condenser circuit replaces the warm make up water used to maintain the tank mass balance in Section 6.2.1. Since the extracted HW has a slightly different temperature compared to the steam heated makeup water, the heat balance used to establish the VHW return temperature constraint in Table 6.5 is affected. The recalculated return temperature constraints for the different seasons are given in Table 6.11.

The maximum flowrate on both sides of heat exchanger VVX7 is taken to be 50 l/s, based on historical operating data. For heat exchangers 11A and 11B, maximum flowrates for the hot sides are taken to be 28 l/s and 70 l/s, respectively, based on exchanger design data.

Table 6.11: Operational parameter constraints for design and operating cases for the mist condenser circuit.

	Mist condenser duty [MW]	Mist condenser HW-outlet [°C]	VHW Return temperature [°C]	VVX7 flowrates [l/s]	VVX11A flowrate (hot side) [l/s]	VVX11B flowrate (hot side) [l/s]
Spring	≤15	86.2	≥95.8	≤50	≤28	≤70
Summer	≤15	86.9	≥87.0	≤50	≤28	≤70
Winter	≤15	86.7	≥95.1	≤50	≤28	≤70

6.4.2 Analysis using the MATLAB-tool

A general methodology is outlined for the MATLAB-tool for the analyses of the different design cases under varying operating conditions. Furthermore, results are presented for every design case for every season. Finally, the best design is motivated and analysed further.

General methodology

In Section 1.1 the need of a general computational tool which can be applied for any heat exchanger network and used to evaluate the effects of changing operating conditions was outlined. The developed MATLAB-tool in this work provides this opportunity and different designs can easily be investigated along with the possibility to directly change operational settings such as bypass ratios and split ratios. By using the MATLAB-tool extensively on the four different network designs general characteristics and optimisation measures can be interpreted from the results.

For all design cases and operating conditions, the analysis using the MATLAB-tool proceeds as follows. First, the sum of the cold water flow (Stream 4 in Figure 6.5) and the blowdown (Supply stream 2 in Figure 6.5) must equal the hot water production required to satisfy the hot water mass balance. Since the only outlet on the secondary heating system side is at Split 2 in Figure 6.5, the flowrate of Stream 2 will then match the required hot water production. The flowrate from blowdown is locked and the supply flow of cold water entering the system is adjusted according to the mass balance outlined in Equation (6.1).

$$\dot{m}_{CW} = \dot{m}_{HW} - \dot{m}_{blowdown} \tag{6.1}$$

The flowrates in the system are controlled by Split ratios 1, 2 and 4. The split ratios are adjusted to always achieve:

- No steam consumption in the internal heating network.
- Design flowrates in the mist condenser (79.8 l/s).

The flowrate to VVX7 is then increased until either constraint occur:

- The flow limit of 50 l/s (given in Table 6.11) is reached.
- The internal heating network starts using steam even with Split ratio 4 at 100 %.

It turns out that the constraint on the mist condenser duty is never reached, because there is not enough heating demand below the mist condenser temperature of about 85 °C. The remaining constraint is the return temperature of the VHW stream. If this temperature is *above* the minimum, the heat content of the VHW is not fully utilised. In this scenario, the flowrate of the closed heating circuit (Stream 5 in Figure 6.5) can be adjusted to shift duty between heat exchanger New1 and VVX7 (and thereby the mist condenser) to optimise overall steam consumption.

If the VHW temperature is *below* the minimum, the UA-value of heat exchanger New1 and the flowrate of the closed heating circuit are adjusted to maximise steam savings while exactly satisfying the VHW temperature constraint given in Table 6.11.

Spring

Operational settings and performance parameters for design cases 1-4 (D1-D4) during spring operation are summarised in Table 6.12. Flow charts for all designs are given in Appendix C. The base case design (BC) achieves steam savings totalling 4.5 MW, as described in Section 6.3.2. All design cases 1-4 can fully utilise the potential of the very hot water, and compensate the hot water lost in the digester section retrofit. Note that designs D1 and D2 use the area of heat exchanger New1 to a higher extent than designs D3 and D4. For D1 and D2, New1 is used without bypass, while bypass is used to reduce the effective UA-value to 32.7 and 34.2 % of the total available for designs D3 and D4, respectively. The UA utilisation is listed in Table 6.12 where a value below 100 % means the exchanger has been bypassed to only utilise part of the available UA-value. As was discussed in Section 6.4.1, designs D3 and D4 do not use heat exchanger New2 but instead move exchangers 11A and B to heat exchange feed water and the VHW stream. The combined size of heat exchangers 11A and B is higher than that of exchanger New2. This means designs D3 and D4 use more of the available heat in the VHW stream for feed water heating and less heat is available for air heating. Consequently, the bypass of exchanger New1 is higher for designs D3 and D4 than for designs D1 and D2. This also explains the lower flowrate on the closed heating water loop (Stream 5 in Figure 6.5). Lowering this flowrate has been observed to shift load from exchanger New1 to exchanger VVX7.

Following the procedure given under "General methodology" in this section, the flowrate of the secondary heating system side of VVX7 was maximised. For all designs, this flowrate can be brought to the maximum value of 50 l/s, given in Table 6.11, without causing steam consumption in the internal heating network.

Table 6.12: Summary of results for spring operation. BC: Base case. D1-D4: Designs 1-4. -S: Spring conditions. The indexation of flowrates and split ratios follow the numbers in Figure 6.5.

	Savings [kW]	MC duty [kW]	VHW return temperature [°C]	VVX New1 UA utilisation [%]	VVX7 flow-rate 6 [l/s]	Closed circuit flowrate 5 [l/s]	SR 1 [%]	SR 2 [%]	SR 4 [%]
BC-S	4500	8998	95.9	100	38.8	38.1	62.7	5.1	50.5
D1-S	6219	9137	95.8	100	50	41.3	48.5	33.3	94.9
D2-S	6595	9514	95.8	100	50	41.5	48.5	33.3	94.9
D3-S	6637	9561	95.8	32.7	50	43.1	48.5	33.3	81.9
D4-S	6340	9253	95.8	34.2	50	38.3	48.5	33.3	81.9

Winter

Operational settings and performance parameters for design cases 1-4 (D1-D4) during winter operation are summarised in Table 6.13. All rows marked WI summarise the performance of a design case using the same operational settings that were used for spring operating conditions. With these operational settings, the hot water production in the mist condenser (Stream 2 in Figure 6.5) will be too low. The deficit is covered by sending warm water to the tank and restoring the tank heat balance by steam heating, and this is accounted for in the listed steam savings. If the VHW return temperature differs from the lower bound in Table 6.11, this will affect the steam required to restore the hot water balance. This has also been accounted for. For rows marked WF, operational settings has been optimised for winter conditions. This means that the operational settings have been adjusted to produce the required amount of hot water and maximise steam savings while satisfying all the constraints given in Table 6.11.

For winter operating conditions, designs D2, D3 and D4 fully utilise the VHW stream. Design D1 can not fully utilise the heat of the VHW stream, even when heat exchanger New1 is used without bypass. Design cases D3 and D4 use heat exchanger New1 to a lower extent compared to designs D1 and D2. This is in agreement with the springtime results listed in Table 6.12 for winter.

For all designs, the flow on the secondary heating system side of exchanger VVX7 is limited by the constraint of not causing steam consumption in the internal heating network (see "General methodology" in this section). This means Split ratio 4 is at 100 % for all final designs.

Table 6.13: Summary of results for winter operation. D1-D4: Design cases 1-4. -WI: Winter conditions, spring settings. -WF: Winter conditions, winter settings. The indexation of flowrates and split ratios follow the numbers in Figure 6.5.

	Savings [kW]	MC duty [kW]	VHW return temperature [°C]	VVX New1 UA utilisation [%]	VVX7 flow-rate 6 [l/s]	Closed circuit flowrate 5 [l/s]	SR 1 [%]	SR 2 [%]	SR 4 [%]
D1-WI	6294	9965	96.0	100	51.9	41.3	48.5	33.3	94.9
D1-WF	7222	12 288	95.1	100	32.4	39.0	71.2	37.3	100
D2-WI	6222	9864	96.4	100	51.9	41.5	48.5	33.3	94.9
D2-WF	7618	12 679	95.1	100	32.4	37.1	71.2	37.3	100
D3-WI	6673	10 315	95.0	32.7	51.9	43.1	48.5	33.3	81.9
D3-WF	7761	12 830	95.1	28.5	41.3	38.3	60.0	44.3	100
D4-WI	6166	9964	94.7	34.2	51.9	38.3	48.5	33.3	81.9
D4-WF	7547	12 618	95.1	24.7	41.3	38.3	60.0	44.3	100

Summer

Operational settings and performance parameters for design cases 1-4 (D1-D4) during summer operation are summarised in Table 6.14. All rows marked SUI summarise the performance of a design case using the same operational settings that were used for the springtime operating conditions. For rows marked SUF, operational settings has been optimised for summer conditions. This means that the operational settings have been adjusted to produce the required amount of hot water and maximise steam savings while satisfying all the constraints given in Table 6.11 for summer.

Despite using heat exchanger New1 without bypass, no design fully utilises the heat content of the VHW, and the stream is returned to the HW-tank at a temperature above the lower bound listed in Table 6.11. The highest steam savings are achieved for Design 3. As was the case for springtime operation, the flow to VVX7 can be brought to the maximum value of 50 l/s without causing steam consumption on the internal heating network.

Table 6.14: Summary of results for summer operation. D1-D4: Design cases 1-4. -SUI: Summer conditions, spring settings. -SUF: Summer conditions, summer settings. The indexation of flowrates and split ratios follow the numbers in Figure 6.5.

	Savings [kW]	MC duty [kW]	VHW return temperature [°C]	VVX New1 UA utilisation [%]	VVX7 flow-rate 6 [l/s]	Closed circuit flowrate 5 [l/s]	SR 1 [%]	SR 2 [%]	SR 4 [%]
D1-SUI	4568	7339	93.2	100	52.2	41.3	48.5	33.3	94.9
D1-SUF	4586	7232	92.7	100	50	45.5	48.5	35.1	50.6
D2-SUI	4837	7551	93.1	100	52.2	41.5	48.5	33.3	94.9
D2-SUF	5022	7332	91.7	100	50	50	48.5	35.1	50.6
D3-SUI	4784	7764	93.9	32.7	52.2	43.1	48.5	33.3	81.9
D3-SUF	5380	7392	90.8	100	50	50	48.5	35.1	50.6
D4-SUI	4509	7579	94.1	34.2	52.2	38.3	48.5	33.3	81.9
D4-SUF	4851	7295	92.1	100	50	50	48.5	35.1	50.6

Further Analysis - Final design

For all operating cases listed in Tables 6.12-6.14, Design D3 achieves the highest steam savings. Since designs D3 and D4 do not invest in a new heat exchanger for feed water heating (as is done in designs D1 and D2), investment costs are lower. This means Design 3 is the most promising option, and this design is chosen for further analysis.

In Table 6.15 the savings of feed water and air heating can be seen for Design 3. For the spring case all the savings correspond to removal of pinch violations. The feed water is not heated with steam utility until 104.0 °C, this implies that the VHW stream heat the feed water to around 1.5 °C above the cold pinch presented in Section 5.4. However, as outlined in Table 6.8 a cross pinch violation of 2.3 MW from heat exchangers K5 and DWL2 in the digester section exists for the base case retrofit. This means that one can go 2.3 MW above the cold pinch and still remove a pinch violation. In this case 335 kW of cross pinch violation is removed for springtime operation. This obviously only accounts for this specific pinch analysis performed with a global ΔT_{min} of 10 °C, if changed to e.g. 8 °C the cold pinch changes to 104.5 °C meaning that no cross pinch violation is removed. During winter and summer nothing specific can be said about pinch removal since the pinch analysis is performed with spring data. However, all temperatures before steam usage for feed water and air are currently below the spring pinch for winter and summer.

Table 6.15: The steam savings for Design 3 for feed water and air heating.

	Steam savings [kW]	
	Feed water heating	Air heating
Spring	4357	1723
Winter	5297	2464
Summer	2497	2883

The results from the runs using the MATLAB-tool provide valuable information when evaluating the network designs. Both limitations and possibilities are highlighted by analysing the utilisation of hot streams, heat exchangers and split ratios.

Analysing the energy savings potential for the different seasons it can be seen that winter and spring use the VHW to its full potential whereas during summer an additional amount of 1300 kW could still be used before returned to the HW-tank. This is due to the lower constraint of 87 °C on the VHW stream. Consequently this extra energy is very hard to utilise and is constrained by temperature differences which currently are lower than 5 °C on both sides of heat exchanger New1. Increasing the flowrate of the closed circuit would increase the temperature difference on both sides of heat exchanger New1 resulting in less need of new additional area to reach the VHW temperature constraint. However, the closed circuit flowrate is currently

maxed out at 50 l/s according to the constraints listed in Table 6.11.

If one instead looks at the utilisation of the heat exchangers for Design 3, it can be seen that the utilisation of New1 is low during both spring and winter operation, corresponding to high bypass ratios (Tables 6.12 and 6.13). This means a significantly lower area investment can be made while still maintaining the same steam savings for winter and spring. If heat exchanger New1 is designed to be used without bypass during springtime operation, the installed UA-value is only 32.7 % of what was used in the original base case design. During winter operation with the operational settings and design parameters listed for Design D3 in Table 6.13, the utilisation of this smaller exchanger would be 87.2 %.

However, reducing the area of heat exchanger New1 leads to a penalty during summer. The new steam savings for summer operation are 4835 kW, corresponding to a steam penalty of 545 kW compared to the original Design 3. The extra investment in area would give enhanced savings during summertime only which makes it harder to motivate. Furthermore, the hours of full production during summertime year 2017 was an average of 54 % for June, July and August as discussed when choosing summer month in Section 5.5.

In the end, cost calculations are outside the scope of this project and therefore no specific comments can be made regarding the pay-back time for the different heat exchanger sizes. It should be noted though that the MATLAB-tool still provide good information for potential pay-back calculations of retrofit suggestions in form of savings and increased/reduced area demands.

6.5 Validation of MATLAB-tool

The heat exchanger UA-values in the case study presented in this chapter are valid for a specification case of spring conditions. As both operating conditions and settings are changed during the case study, a correction factor is used to update UA-values for changes in flowrates. The correction factor is derived in Section 2.2.2. Section 6.5.1 below includes a validation of the correction factor used in the MATLAB-tool, comparing it to a more advanced model developed by Södra engineers.

In Section 6.5.2, the results of the final design in the case study in Section 6.4.2 are compared for runs with and without correction factor. This gives an estimate on how sensitive the predictions by the MATLAB-tool are to the precision of the correction factor.

6.5.1 Södra model

The correction factor presented in Section 2.2.2 is used for the network calculations in the case study presented in this chapter. An analysis of a sub-network of the mist condenser circuit is used to asses the accuracy of this correction factor and,

in extension, of the MATLAB-tool. The network is visualised in Figure 6.6. This network is analysed both using the MATLAB-tool and a more advanced process model developed by mill engineers at Södra Cell Mönsterås. The Södra model is run for a dimensioning case and exchanger UA-values, as well as properties required to calculate the correction factor described in Section 2.2.2, are extracted from the model output. These properties are given as input to the MATLAB-tool. For validation of the MATLAB-tool, both the Södra model and the MATLAB-tool are run for two additional validation cases, and the results are compared.

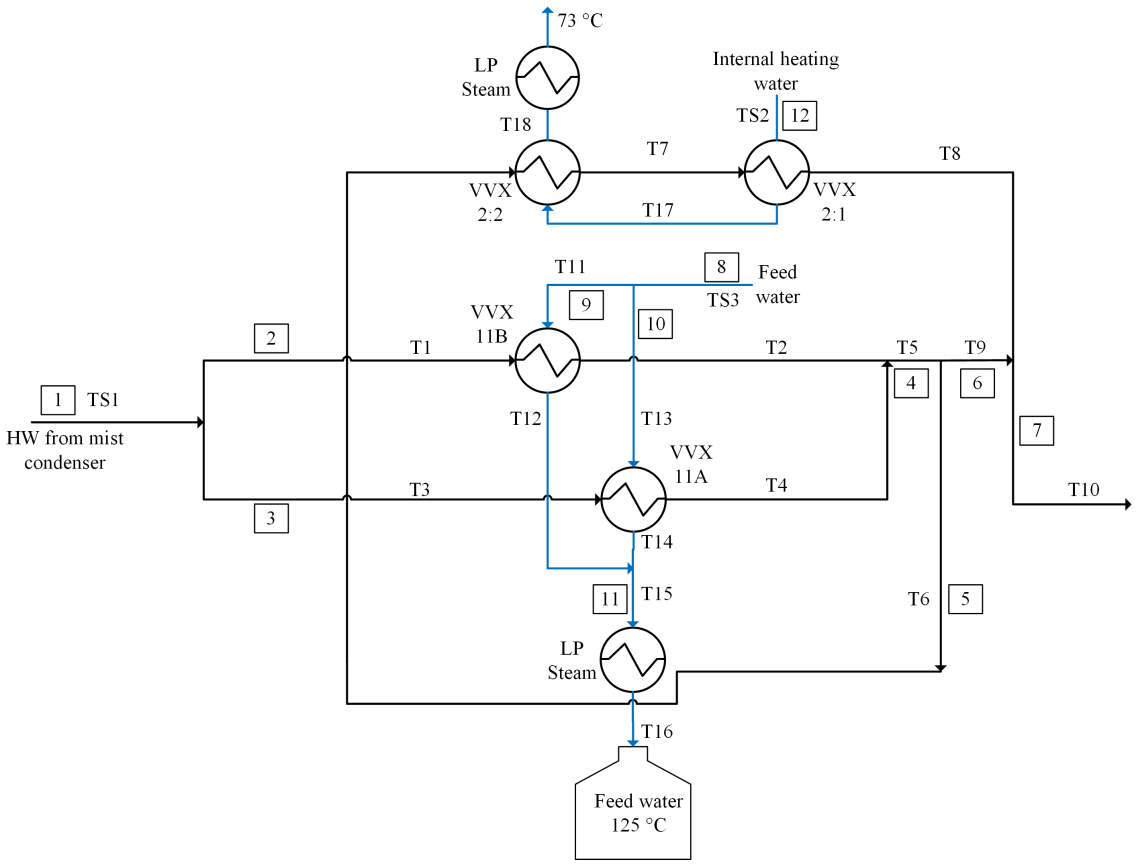

Figure 6.6: An overview of the validation network used to compare the MATLAB-tool with the Södra model. Numbers within boxes represent the stream numbering and T# the temperature numbering.

The operating conditions used for the dimensioning case (D) represent spring/autumn conditions and the two validation cases (V1 and V2) represent summer and winter and all are summarised in Table 6.16. The UA-values predicted by the MATLAB-tool and the Södra model for the two validation cases are compared in Table 6.17. For reference, a case where the MATLAB-tool is run without the UA correction factor (i.e., with UA-values maintained from the dimensioning case), is included in the comparison.

Table 6.16: The operating conditions used for dimensioning exchangers in the MATLAB-tool (D) and for validation against Södra's model (V1 and V2). Stream and temperature numbering according to Figure 6.6.

	Flowrates [l/s]						Supply temperatures [°C]		
	2	3	5	9	10	12	TS1	TS2	TS3
D	25	22.5	21.4	35.4	18.5	29.5	86.8	51.4	82.2
V1	27	18	13.5	29.3	18.2	28.7	86.8	62.9	85
V2	38.7	20.8	59.5	37	23	58	87	45.4	76.2

Table 6.17: Comparison of UA-values predicted by the MATLAB-tool and the Södra model. The given numbers are the percentage deviation of the MATLAB value compared to the value of the Södra model. Columns marked "Corrected": MATLAB-tool is run with correction factors. "Uncorrected": MATLAB-tool is run without correction factors.

	V1		V2	
	Corrected	Uncorrected	Corrected	Uncorrected
11A	-3.9 %	+2.8 %	+2.3 %	-2.1 %
11B	-1.5 %	-0.3 %	+1.3 %	-14.3 %
VVX2:1	-2.6 %	+23.3 %	+6.5 %	-40.9 %
VVX2:2	-2.0 %	+21.0 %	+6.1 %	-37.1 %

Flowrates in the heat exchangers are generally lower in verification case V1 than in the dimensioning case D (Table 6.16). This means UA-values will be lower for case V1. As is seen in Table 6.17, the corrected MATLAB-tool predicts a lower UA-value than the Södra model. Consequently, the MATLAB-tool overestimates the change in UA-value.

For verification case V2, flows are higher than for the dimensioning case. The UA-values predicted by the corrected MATLAB-tool are now higher than those predicted by the Södra model. Again, this means the change in UA-value is overestimated by the MATLAB-tool. However, the convergence tolerance of the Södra model is +-5 %. This means the overestimation is in most cases within the same precision interval as the convergence criteria for the Södra model. Thus, the precision of the correction factor used for the designs in Section 6.4 is in line with the model developed by Södra and is considered satisfactory for a tool used for early design evaluations.

An incorrectly predicted UA-value ends up in an overestimation or underestimation in terms of steam usage. The effect on steam usage using uncorrected values compared to corrected is presented in Section 6.5.2 below.

6.5.2 Case study

To get more information about the impact of the correction factor the final design from the case study, Design 3 (visualised in Figure C.3), is calculated without the correction as well.

For this network the Södra model can not be used since modelling data is not available for the additional heat exchangers. For analysis in this section, the dimensioning case used for calculating UA-values and correction factors is springtime operation of the current mist condenser circuit, visualised in Figure 6.5, i.e., the same dimensioning case as is used in the case study. The results can be seen in Table 6.18. The runs without correction factor use the exact same operating conditions and settings as the original run of Design 3.

Table 6.18: Comparison of parameters with and without correction factor for Design 3. The values in the table are uncorrected and the percentage is relative to the corrected values. The temperature difference is absolute. The values for the corrected cases can be seen in Table 6.12, 6.13 & 6.14.

	Savings [%]	**MC duty** [%]	**VHW return temperature** [°C]	**UA-value VVX11A** [%]	**UA-value VVX11B** [%]	**UA-value VVX2:1** [%]	**UA-value VVX2:2** [%]	**UA-value VVX7** [%]
D3-S	-3.9	-0.6	0.5	-5.8	-17.2	6.0	5.3	-9.3
D3-WF	-5.4	-0.7	1.0	-10.0	-23.5	-6.3	-5.7	-1.8
D3-SUF	-1.6	-1.2	-0.1	-1.5	-12.7	37.7	33.3	-13.0

Analysing the predicted steam savings in Table 6.18, it can be seen that these are 1.6 % to 5.4 % less without the correction factor. Most of this is due to the fact that design D3 uses the VHW stream, rather than the secondary heating water from the mist condenser, on the hot side of VVX11A & B. The VHW flowrate is higher than the dimensioning flowrate. Without the correction, the associated increase in UA-values is not accounted for. On the cold side, i.e. the feed water side, the spring case uses the dimensioning flowrate. However, the winter flowrate is higher, leading to further underestimation of the UA-values of exchangers 11A& B. The summer cold side flowrate is lower than for the dimensioning case, partly counteracting the effect of the increased flowrate on the hot side.

Predicted steam savings are not very sensitive to the UA-value of VVX7, since an overestimated UA-value here will shift duty from New1 to VVX7, and vice versa for an underestimated UA-value. The effect on the combined duty will be minor. Regarding VVX2:1 and VVX2:2, operational settings are adjusted during the case study to give zero steam consumption in the internal heating network, using corrected UA-values. This means deviations in UA-values for VVX2:1 and 2:2 will only have minor impact on overall steam savings.

A similar analysis was performed by Persson and Berntsson [16] where the same correction factor was used to update UA-values for changes in operating conditions. In their work the estimated energy savings differed by less than 1 % for calcula-

tions with or without the correction factor. The impact of the correction factor in this analysis is slightly higher. This is most likely because Persson and Berntsson analysed the impact of the correction factor for an entire mill for monthly averages whereas this analysis is for a smaller sub-network for a smaller extracted data set.

In conclusion, the correction factor is a useful correlation which makes the MATLAB-tool more representative and precise during the analysis of changing operating conditions or settings in a heat exchanger network. However, it should be noted that individual heat transfer coefficients are needed when implementing the correction factor for a specification case. If this data is not available the tool is still considered useful for estimating steam savings in an early design phase, since the difference in estimated savings is small with or without the correction factor.

7
Discussion

The discussion is divided into two areas, of which the first focuses on the MATLAB-tool and the second on the case study. The first section discusses the benefits of using the MATLAB-tool during heat exchanger network design, using examples from the case study. Limitations and uncertainties of the tool are also discussed. The second section discusses the practical feasibility of the proposed retrofit designs and the need for improved pinch analysis and process mapping.

7.1 MATLAB-tool

The Introduction (Chapter 1) of this report mentions the importance of accounting for structural flexibility when evaluating the performance, in terms of steam savings, of a heat exchanger network design during varying conditions. This means a fair performance evaluation should include a tuning of operational settings (split ratios, bypass ratios and similar) to adapt the network to changing conditions. The MATLAB-tool which was developed within the frames of the project, using the theoretical outline given in Sections 2.2.1-2.3.1, allows such performance evaluation. The tool can be applied to any heat exchanger network and operating conditions are easily changed. Operational settings can then be fine tuned to suit the new conditions.

The importance of accounting for the structural flexibility of a heat exchanger network is illustrated by Tables 6.13 and 6.14. Firstly, the steam savings for all designs can be improved by adjusting operational settings. This is most evident for Designs D2 and D4 during winter conditions, where steam savings are 22.4 % higher when operational settings are adjusted to suit the new conditions, compared to when settings for spring time operation are maintained. Secondly, the ranking of the designs, in terms of steam savings, is different before and after adjusting operational settings. For spring conditions, the designs are ranked 3-2-4-1, as can be seen in Table 6.12. The final operating cases for summer and winter are ranked in the same order (Tables 6.13 and 6.14). However, in the initial operating cases for winter and summer, the ranking is different. For example, Design D2 performs better than Design D3 during summer conditions and Design D2 is ranked worse than Design D1 for winter conditions, if spring time operational settings are maintained.

While the MATLAB-tool offers a way of accounting for the structural flexibility

of heat exchanger networks when different design options are compared, it does not give any explicit or quantifiable information on that flexibility. On the other hand, something can in fact be said about the *relative* structural flexibility of the designs investigated in this work. If flexibility is defined as the ability of a network to reach target temperatures under changing conditions, then all the investigated designs have sufficient flexibility, since they can all reach target temperatures under all investigated conditions. If total flexibility is seen as the combination of energy flexibility and structural flexibility, high utility consumption, i.e. a high demand for energy flexibility, can be seen as a penalty for low structural flexibility. Using this reasoning, Design D3 can be said to be the design with higher structural flexibility.

A similar way of comparing the structural flexibility of networks is to compare how well they utilise the very hot water (VHW) generated in the digester section retrofit, described in Section 6.2. If this water is used down to the lowest allowed temperature (Table 6.11), the investment in the digester section retrofit is used to the highest possible extent. By comparing Tables 6.12-6.14 to Table 6.11, it can be seen that all designs make full use of the VHW during spring and winter conditions. During summer conditions, the situation is quite different and no design is able to make full use of the VHW. However, the utilisation is highest for Design D3 and, consequently, ranking the designs by VHW utilisation will again result in Design D3 being the best choice.

Beyond providing a way to account for structural flexibility in performance evaluations, the MATLAB-tool can help identifying oversized or undersized exchangers. In the case study, this is illustrated by exchanger New1 (see Tables 6.12 and 6.13). If one of the new exchangers in a prospected design is bypassed for a majority of investigated conditions it may be worthwhile to install it with less area. Installing the exchanger with less area means reduced capital costs but no utility penalty under conditions where it was previously bypassed. A penalty will however be present under conditions where area utilisation of the new exchanger is high. Similarly, a heat exchanger which is used without bypass at a majority of conditions is a candidate for increased area. In such situations, there may exist direct trade-offs between capital cost for structural flexibility and utility consumption for energy flexibility. The MATLAB-tool offers a direct way to investigate the effect of changed exchanger area and, in extension, the trade off between utility and capital for a specified level of flexibility. However, cost data is required and such analysis is not included for exchanger New1 in this project.

It is worth noting that a trade-off between capital and energy does not necessarily exist, i.e. that higher structural flexibility does not necessarily entail higher capital costs. In the case study performed in this work, design D3 has the same investment level as design D2, but performs better at all operating conditions. Similarly, designs D2 and D3 both perform better than D1 and D4 despite higher investment levels for the latter two designs. In fact, steam savings are 6.7-17.3 % higher for the best design (D3) than for the worst (D1), depending on season. By being able to analyse several structurally different designs for varying conditions already in the

early design phase, designs which achieve a specified level of flexibility at low capital and energy costs can be identified. Such analyses are greatly facilitated by the generality and fast calculations of the developed MATLAB-tool.

Note that, even if only one set of operating conditions is considered in design, the MATLAB-tool can be used to find operational settings which improve the performance of an investigated design. This is illustrated by the improvements made to the base case design BC in order to arrive at Design D1. The two designs are compared in Table 6.12. The two designs use the same units and the same network structure, and the only difference is the possibility to send HW to the HW-tank in Design D1. By this change and by adjusting operational settings, the steam savings are increased by 1.6 MW in Design D1.

The developed MATLAB-tool achieves some important benefits of a simulation tool, such as rapid calculations and a possibility to easily evaluate the effect of new operating conditions and settings. Furthermore, it is easily applicable to any network structure, meaning a case can be investigated without the need of building a simulation model. To achieve these benefits, some properties of a more rigorous simulation tool have been sacrificed. All temperature dependency is ignored and actual fluid properties can not be used. Instead, a stream is characterised by a constant heat capacity flowrate. Without fluid properties, neither individual heat transfer coefficients nor overall U-values can be calculated. Instead, UA-values are set for a specification case and updated using the correction factor described in Section 2.2.2. This allows updating UA-values for flowrate changes and the correction is found accurate for the case study performed in this work, see Section 6.5. However, problems may arise if an exchanger is used far outside the temperature interval which was used for dimensioning, since the correction factor does not account for the effect of temperature deviations from the dimensioning conditions.

A related issue, also arising from the fact that fluid properties are assumed independent of T, is that no good way to represent streams with varying CP-values exists. For example, piece-wise linearisations of CP-values can not be included since network temperatures would then have to be known before solving the equation system representing the heat exchanger network.

7.2 Case study

The digester section is retrofitted as described in Section 6.2 to partly produce VHW instead of HW. In order to do so, structural changes are required which place heat exchangers in series that were previously in parallel. This change makes the network more vulnerable towards disturbances and process streams must always be sufficiently cooled in order to avoid operational stops. Therefore, bypass possibilities must exist for all the heat exchangers on the VHW stream so service can be done while in operation. Another issue with the retrofit regards pumping. Placing heat exchangers in series leads to a higher pressure loss compared to parallel placement. After the retrofit two additional heat exchangers are also added on the VHW-stream

inside the mist condenser circuit in form of New1 and VVX11A&B (or New2). This will lead to a probable additional pump investment for the retrofit to work satisfactorily.

During calculations for Retrofit 2, a flowrate of 79.8 l/s through the mist condenser was considered for all cases. During some operating conditions this could lead to unnecessary pumping costs. Analysing Table 6.14 for summer conditions, it can be seen that SR 4 is only at around 50 % for all designs and the flowrate down to VVX7 is at its maximum value according to the constraint in Table 6.11. This implies that roughly 12.5 l/s of HW is re-circulated and brought back to the mist condenser. If reducing the flowrate in the mist condenser by 12.5 l/s SR 4 can be opened to 100 %. However, this would obviously also make the system more vulnerable towards short-term disturbances which increase the duty of VVX2:1 and 2:2.

The closed circuit flowrate, as shown in Table 6.11, is limited to 50 l/s based on analysis of historical high operational flows. In the retrofit, an additional heat exchanger New1 is added to the circuit. It is worthwhile considering that if the pump was previously running at its maximum capacity, an additional heat exchanger will increase the pressure drop in the closed circuit. This means that in reality the flow constraint would need to be lower to avoid investing in a new pump. However, it can be seen by analysing the flowrates in Table 6.12-6.14 that 50 l/s is only used in the closed circuit during summer. As all designs during summer is close to 50 l/s, the absolute savings will decrease the same amount for a decreased flowrate. Thus, the outcome of the steam saving ranking between the designs for summer will not change.

In Section 5.4 the actual and minimum heating demand from the pinch analysis is demonstrated in Table 5.3. The difference is 27.7 MW and the majority of the heating demand is represented by stream C9-C17 in Table 5.2 as aggregated steam demands due to insufficient mapping. If it is possible to decouple the aggregated steam demands and identify the specific steam consumers, a lower minimum heating demand could possibly be achieved. This would increase the amount of potential savings available in the system. Findings of specific steam consumers would have to be below HW-tank temperature for heating by the secondary heating system to be possible. As of now the cold pinch point is 102.5 °C which implies that there is a gap between the highest tank temperature (85 °C) and the cold pinch. In this work a VHW stream was created to replace steam usage in this specific gap. However, the VHW stream is fully utilised and if more findings show steam usage between 85 °C and the cold pinch, more VHW must be generated or other solutions, such as direct process to process heat exchange, must be found.

It should be noted that the flue gases from the recovery boiler have both the temperature and flowrate necessary to be used both for either feed water or air preheating. However, retrofit solutions involving the flue gases have already been investigated by mill engineers, and been rejected on the basis of techno-economic considerations. Therefore, proposals involving flue gases have not been investigated in this work.

8

Conclusions and Future Work

This project has focused on evaluating and improving structural flexibility and performance of heat exchanger networks, under varying operating conditions. To achieve this, a general MATLAB-tool has been developed. This tool can be applied to any network structure and the effects of varying operating conditions and operational settings can easily be investigated. This allows identifying heat exchanger networks which are energy efficient during a range of operating conditions.

The MATLAB-tool offers a way to account for structural flexibility of network designs when their performance, in terms of utility consumption, is evaluated for multiple sets of operating conditions. The importance of this has been demonstrated in the case study, where tuning of operational settings increases steam savings by up to 22.4 % when changing between operating conditions. By providing an easy way to evaluate the effect of tuning operational settings, the full potential of early designs, which may otherwise have been overlooked, can be realised. This increases the possibility of arriving at the best possible design.

In the performed case study, four heat exchanger network designs were investigated. The best design achieved steam savings of 6.6, 7.8 and 5.4 MW, for spring, winter and summer conditions, respectively. These savings are 6.7, 7.4 and 17.3 % higher than for the worst design. All designs achieved the required level of flexibility, but the best design used less new units and required lower utility consumption. This implies that a trade-off between flexibility, capital and energy does not necessarily exist in retrofit projects.

Potential trade-offs between energy and capital costs for required flexibility can be identified using the MATLAB-tool. By investigating various operating conditions, prospected heat exchangers which are consistently under-utilised can be identified and the effect of installing them with smaller areas can be investigated. Similarly, candidates for increased size can be identified.

To increase the usefulness of the MATLAB-tool, future work should add a possibility to handle streams with varying CP-values. This may require iterative solutions. While the tool is accurate for the system investigated in this work, further verification is necessary. Specifically, the effect of using a heat exchanger outside of its dimensioning temperature intervals should be investigated in comparison to rigorous simulation tools. It is also of interest to investigate fluids where the product of heat capacity and density show a more significant temperature dependency than for

water, to test the impact of the assumption of constant CP-values.

Furthermore, a future project would be to connect optimisation algorithms to the developed MATLAB-tool. Current optimisation process is performed by manual iterations and sensitivity tables. A general algorithm would make it possible to relax constraints and open up for further optimised solutions which possibly could have been over looked before.

Regarding this and future energy efficiency projects at Södra Cell Mönsterås, some conclusions can be made from the current pinch analysis. The performed pinch analysis shows that there exist a potential saving of 27.7 MW. In the case study the retrofit with highest savings removes 6.6 MW of the total pinch violations during spring. To give a correct view of the actual removed pinch violations for the whole year, a pinch analysis should be performed for each season. In order to realise more energy efficiency projects at the mill in the future, a more extensive mapping of the process streams is needed. Currently, 84.5 % of all the steam demand is found as aggregated streams. By decoupling aggregated steam demands in sectors such as drying and bleaching, further pinch violations might be identified.

Bibliography

[1] Swedish Energy Agency, "Energieffektiviseringsdirektivet", 2017. [Online]. Available:
http://www.energimyndigheten.se/energieffektivisering/lag-och-ratt/energieffektiviseringsdirektivet/

[2] Swedish Energy Agency, "Sektorstrategier för energieffektivisering", 2017. [Online]. Available:
http://www.energimyndigheten.se/energieffektivisering/program-och-uppdrag/Sektorsstrategier-for-energieffektivisering2/

[3] Swedish Energy Agency, "Energiläget 2017", 2017. [Online]. Available:
https://energimyndigheten.a-w2m.se/Home.mvc?ResourceId=5693

[4] Sodra, Sweden, "Södra Cell Mönsterås", 2016. [Online]. Available:
https://www.sodra.com/en/pulp/production/monsteras/facts-about-sodra-cell-monsteras/

[5] Sodra, Sweden, "Resource efficiency", 2016. [Online]. Available:
https://www.sodra.com/en/about-sodra/sustainability/strategy-for-sustainability/resource-efficiency/

[6] Chalmers University of Technology, "Flexible process integration solutions for the pulp and paper industry", 2017. [Online]. Available:
https://research.chalmers.se/en/project/7314

[7] F. Nihlmark, M. Mahmoud, "Analysis of the secondary heating system of Södra Cell Mönsterås", MSc Thesis, Department of Space, Earth and Environment, Chalmers University of Technology, Göteborg, Sweden, 2017.

[8] I. C. Kemp, *Pinch Analysis an Process Integration: A User Guide on Process Integration for the Efficient use of Energy. 2*nd ed., Oxford, UK: Butterworth-Heinemann, 2007.

[9] R.E. Swaney, I.E. Grossmann, "An index for operational flexibility in chemical process design. Part I: Formulation and theory", *AIChE Journal*, vol. 31 (4), pp. 621-630, 1985.

[10] F.V. Lima, Z. Jia, M. Ierapetritou, C. Georgakis, "Similarities and differences between the concepts of operability and flexibility: The steady-state case", *AIChE Journal*, vol. 56 (3), pp. 702-716, 2010.

[11] T. Larsson, S. Skogestad, "Plantwide control - a review and a new design procedure", *Modelling, Identification and Control*, vol. 21 (4), pp. 209-240, 2000.

[12] S.K. Chodavarapu, A. Zheng, "A definition of steady-state plantwide controllability", *Industrial & Engineering Chemistry Research*, vol. 41 (17), pp. 4338-4345, 2002.

[13] J. Cerda, M. R. Galli, N. Camussi, M. A. Isla, "Synthesis of flexible heat-exchanger networks: I. convex networks", *Computers & Chemical Engineering*, vol. 14 (2), pp. 197–211, 1990.

[14] E. Kotjabasakis, B. Linnhoff, "Sensitivity tables for the design of flexible processes (1) - How much contingency is cost effective?", *Chem Eng Res Des*, vol. 64 (3), pp. 197-211, 1986.

[15] SA. El-Temtamy, "Flexible Heat Exchanger Networks", *Chem Eng*, vol. 118 (4), pp. 32-38, 2011.

[16] J. Persson, T. Berntsson, "Influence of Seasonal Variations on Energy-Saving Opportunities in a Pulp Mill", *Energy*, vol. 34 (10), pp. 1705-1714, 2009.

[17] R. Smith, *Chemical process design and integration. 2*nd ed., Chichester, UK: Wiley, 2016.

[18] R. K. Sinnot, *Coulson and Richardson's Chemical Engineering Volume 6: Chemical Engineering Design 4*th ed., Oxford, MA: Elsevier, 2005.

[19] R. K. Shah, D. P. Sekulić, *Fundamentals of Heat Exchanger Design*, Hoboken, N.J.: Wiley, 2003.

[20] P. Bokinge, D. Erlandsson, "HEN-S - User Manual", unpublished.

[21] S.Harvey, *Industrial Energy Systems*, Course book produced at the Department of Energy Technology at Chalmers University, 2016.

[22] Swedish Meteorological and Hydrological Institute (SMHI), "Års- och månadsstatistik", 2018. [Online]. Available: `https://www.smhi.se/klimatdata/meteorologi/2.1240`

A

Description of stream changes

Every stream explained and compared to the stream list created by N&M. Number in parentheses is the stream number(s) used by N&M for the same stream(s).

A.1 Hot streams

H1: Surface condensers in evaporation section 1. Duty recalculated from SHS-side. This gives a minor change compared to the duty listed by N&M.

H2: Surface condensers in evaporation section 2. Duty recalculated from SHS-side. This gives a minor change compared to the duty listed by N&M.

H3: LO (Oxygen liquor) is cooled by the secondary heating system before being supplied to a process stage (tvättpress). No changes from N&M.

H4 (H21): Cooling of oxygen liquor tank. No changes from N&M.

H5 (H4): Mist from green liquor production. Essentially a moist air stream at high temperature which is cooled and condensed in a "Mist condenser" before being vented to the atmosphere. Start and target temperatures are SHS-side values. The sensor used by N&M for the inlet temperature on the SHS side was not correct. The temperature has been updated from 54.6 °C to 59.2 °C. The available heat content of the mist has been set to 15 MW after consultation with mill engineers. However, all of this is not utilised in current operation.

H6 (H5 and H7): Liquor condensate from evaporation plant, currently used in bleaching section. This stream is present as two segments in N&M: H5 and H7. N&M set a hard target equal to the temperature where the condensate is currently used. However, this stream is merely a hot water stream and any other hot water stream could be used in its place. In this work, it is instead treated as an available heat source at the condensate tank temperature and given a soft target of 15 °C.

H7 (H6,H14,H18): Thin liquor outlet from secondary flash in digester section. Cooled before being supplied to evaporation. The TL passes two deduction liquor exchangers (DWL1/2) in parallel in the digester section, and are then mixed. The mixed stream is then cooled further in Liquor coolers 1+2 (series) to the target temperature of 95.6 °C. N&M treated this as three separate streams (one for each

exchanger). These have been merged to one stream in this work.

H8 (H22): PO-gas (essentially: moist air) is vented from a tank and heat exchanged. This stream is currently used for heating of both the sawmill heating network and the external (Mönsterås) heating network (in that order). N&M estimated enthalpy change and temperatures for this stream based on data for the sawmill heating network, thus excluding the external heating network. By including both the sawmill and the external heating network in the estimate, the estimated enthalpy and target temperature is changed. The change is very minor: enthalpy drop increases from 2.3 MW to 2.4 MW and the target temperature changes from 96 to 95.6 °C.

This stream should be given a soft target and a piecewise linearisation for CP. However, the available data is not enough to do so. Instead, a hard target is kept and CP is taken constant in the small temperature interval (100 to 95.8 °C).

H9: BSO from "Liquor tank pressure diffusers". Cooled before being used in process (supplied to high pressure feeder). Values kept from N&M.

H10: BSO from "Liquor tank pressure diffusers" is cooled and recirculated to the tank. This stream represents cooling of the tank. The target temperature is changed from N&M, since it is a manual measurement an additional 6.4 % is added to the measured value.

H11 (H16): Cooking liquor from the primary flash stage in the digester section. Cooled in two parallel exchangers (K4 and K5) and sent to high pressure feeders. All values kept from N&M.

H12 (H23 and H17): Flash vapor from digester section flash tanks. This is condensed in two parallel exchangers ("Flash steam condenser" and "Sawmill condenser"). The duty of the exchangers was estimated by N&M based on the SHS side.

The duty for the sawmill condenser is kept from N&M. However, an error regarding the SHS flowrate used to estimate the flash steam condenser duty was found. The duty has been updated to 6687 kW (6100 kW in N&M).

The condensation temperature has been set to equal the vapour inlet temperature.

H13 (H12): Condensation of vapor from the degassing vessel in digester 4/5. Changed to constant temperature condensation (at inlet T).

H14 (H11): Condensation of vapor from digester 6. Changed to constant temperature condensation (at inlet T).

H15 (H8): This stream is a mixture of remaining vapor after streams H12-H14 have been condensed in their respective first condensation step. After mixing, the

uncondensed gases are condensed in a subsequent exchanger. Ideally, this stream should be merged to streams H12-H14. However, this has not been possible to achieve why it is treated as a separate stream. Condensation temperature changed to constant at inlet T.

H16 (H13): Cooling of condensate after condensation of H12. After cooling, this stream is sent to decanting. No changes made from N&M.

H17 (H15): BSO-flow leaves from top of K6 pressure diffuser, is then cooled and mixed with a flow from a filtrate tank. After this, returned to the bottom of the pressure diffuser. No changes.

H18 (H19): BQ1 back water which is used to heat the external heating network, the sawmill heating network and feedwater, before being discharged. The flowrate has been changed to match the load 10+12.3 MW (Sawmill+external) with same tank temperature (86.7) and temperature after sawmill (71.7). This gives a flowrate of 355.66 l/s. (This means the temperature between external and sawmill changes to 79.97).

H19 (H20): BPO-backwater taken from tank to heat feedwater and thereafter returned to the tank (the recirculating BPO stream is cooled to maintain the temperature of the BPO-tank). Because of a typo in N&M the target temperature is changed from (85,6->86,5) to match their measurements. Mass flow and duty is re-calculated and updated.

H20 (H24): Flue gases from recovery boiler. This stream data is taken directly from N&M, the heat capacity of air is used for flue gases, considered ok since it is on the conservative side.

H21 (H26): Moist air from the drying section. No information on relative humidity is given in N&M. If a humidity of 100 % is assumed at the current outlet, the available duty can be estimated to 30.9 MW using psychrometric charts and the start and target temperatures given by N&M.

H22 (New): Condensate (clean) from a condensate tank is cooled before being supplied to the feedwater buffer tank.

A.2 Cold streams

C1 & C2 (C1, C2, C3, C4, C18): The feedwater sent to the recovery- and power boilers are from two different sources: make up and recycled condensate. N&M only included the make up water. Further, the stream was divided into one segment per exchanger used in the heating. In this work, two streams are used: one represents the make up water (C2) and one the recycled condensate (C1). For the make up

water, the start temperature is changed from 30.9 to 8.3 °C. For the recycled condensate, the start temperature is set to 31.4 °C.

C3 (C10, C5): N&M used engineering estimates for the combustion air start and target temperatures. N&M assumed that APH was done only by the LP/MP consumed in the recovery boiler, and calculated duty and mass flowrate based on this.

In fact, APH is also done using hot water produced in VVX 7 (C5 in N&M).

Further, both start and target temperatures, as well as volumetric air flow is available in INFOPLAN. The start temperature has been changed and the mass flow is now from INFOPLAN, i.e. not calculated to fit the steam consumption (duty). Instead, the duty is now calculated based on flowrate and start and target temperatures from INFOPLAN.

C4 (C9): Sawmill heating network. All data directly from N&M.

C5 (C6): Warm water consumption. Flowrate unknown. The flowrate given by N&M is not trusted: there is no clear description of how the flowrate is found, and additional branches have been added to the flow chart established by N&M. This flow is now taken as the sum of causticization, försileri, bleaching and tätningsvvx.

C6 (C7): Process demand of hot water. The flowrate given by N&M can not be reproduced and has been updated. The flowrate is calculated from pump operating parameters by process engineers.

C7 (C8+H7): Process demand of 90 °C water. The flowrate given by N&M can not be reproduced and has been updated. The flowrate is calculated from pump operating parameters by process engineers.

C8 (New): Internal heating network. Not included as a cold stream in N&M but all required data was available and has been taken from N&M.

C9 (C20): Steam consumption in the drying section. This was represented by N&M as a stream with specified start and target temperatures, and flowrate. To achieve this they assumed that all steam consumption in the drying section was for preheating of air to the drying machines. However, steam is used both for air heating and in the actual drying machine. The two uses can not be disaggregated with the available data. In this work, the drying section is therefore treated as a black box steam consumer with a temperature equal to the condensation temperature of the used steam, shifted down by ΔT_{min}.

C10-C17 (C11-C17, C19): Various black-box steam demands taken from N&M. Temperatures changed to match the actual condensation temperatures (minus ΔT_{min}). Previously, the temperature was based on the superheated temperature of the used steam.

Duties corrected: N&M found steam flowrate and calculated steam demand (MW) by assuming a condensation temperature of 0 °C (i.e., steam is condensed and cooled to 0 °C). This has been changed to 125 °C, meaning all steam demands have been decreased.

B

Relationships for thermal effectiveness

The thermal effectiveness is demonstrated for the true counter-current heat exchanger and also of a shell-and-tube heat exchanger. Thermal effectiveness for the listed heat exchangers in Chapter 4 and much more is found in the book "Fundamentals of Heat Exchanger Design" by Shah [19].

B.1 Counter-current heat exchanger

Looking at the counter-current heat exchanger configuration in Figure B.1, indexation 1 and 2 could be either hot or cold. Which one that is what does not matter for the outcome of the calculations. If thermal effectiveness, P, is obtained for one side the relations in Equation (2.10) can be used to get the other one.

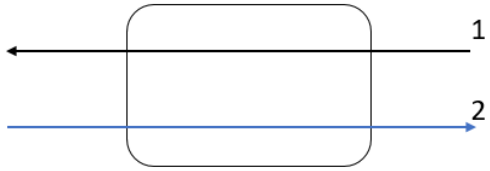

Figure B.1: Counter-current heat exchanger. 1 and 2 could be either hot or cold.

For unknown thermal effectiveness:

$$P_1 = \frac{1 - exp[-NTU_1(1 - R_1)]}{1 - R_1 exp[-NTU_1(1 - R_1)]} \tag{B.1}$$

If R=1

$$P_1 = \frac{NTU_1}{1 + NTU_1} \tag{B.2}$$

For known thermal effectiveness:

$$NTU_1 = \frac{1}{1 - R_1} ln \frac{1 - R_1 P_1}{1 - P_1} \tag{B.3}$$

If R=1

$$NTU_1 = \frac{P_1}{1 - P_1} \tag{B.4}$$

B.2 Shell-and-tube heat exchanger

Looking at the shell-and-tube heat exchanger configuration in Figure B.2, indexation 1 and 2 could be either hot or cold. In this case number 1 is allocated to the shell side of the heat exchanger. If the thermal effectiveness, P, for tube side is wanted one use the relations in Equation 2.10. This also mean that the heat capacity flowrate, R, could either be R_h or R_c according to Equation 2.8 and 2.9.

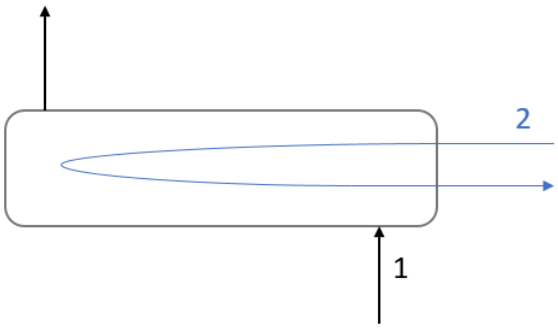

Figure B.2: 1-2 TEMA E shell-and-tube heat exchanger with index 1 on shell side.

For unknown thermal effectiveness:

$$P_1 = \frac{2}{1 + R_1 + Ecoth(ENTU_1/2)} \qquad E = (1 + R_1^2)^{1/2} \tag{B.5}$$

If R=1

$$P_1 = \frac{1}{1 + coth(NTU_1/\sqrt{2})\sqrt{2}} \tag{B.6}$$

For known thermal effectiveness:

$$NTU_1 = \frac{1}{E} ln \frac{2 - P_1(1 + R_1 - E)}{2 - P_1(1 + R_1 + E)} \tag{B.7}$$

if R=1

$$NTU_1 = ln \frac{2 - P_1}{2 - 3P_1} \tag{B.8}$$

C

Retrofit designs

This appendix includes flow charts of the four mist condenser circuit retrofits investigated in this work. The numbering follows that given in Table 6.9.

Design 1:

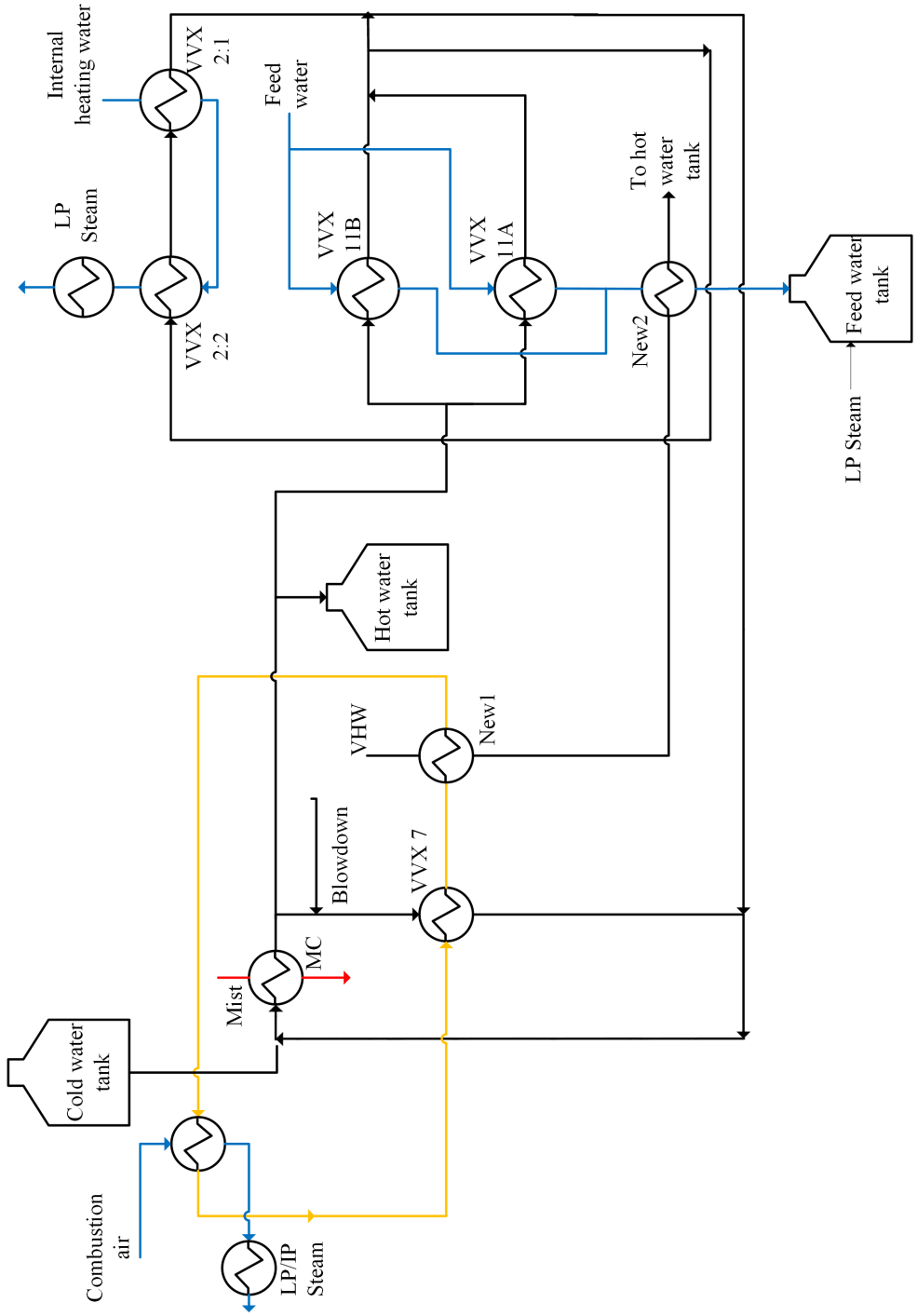

Figure C.1: Design 1

Design 2:

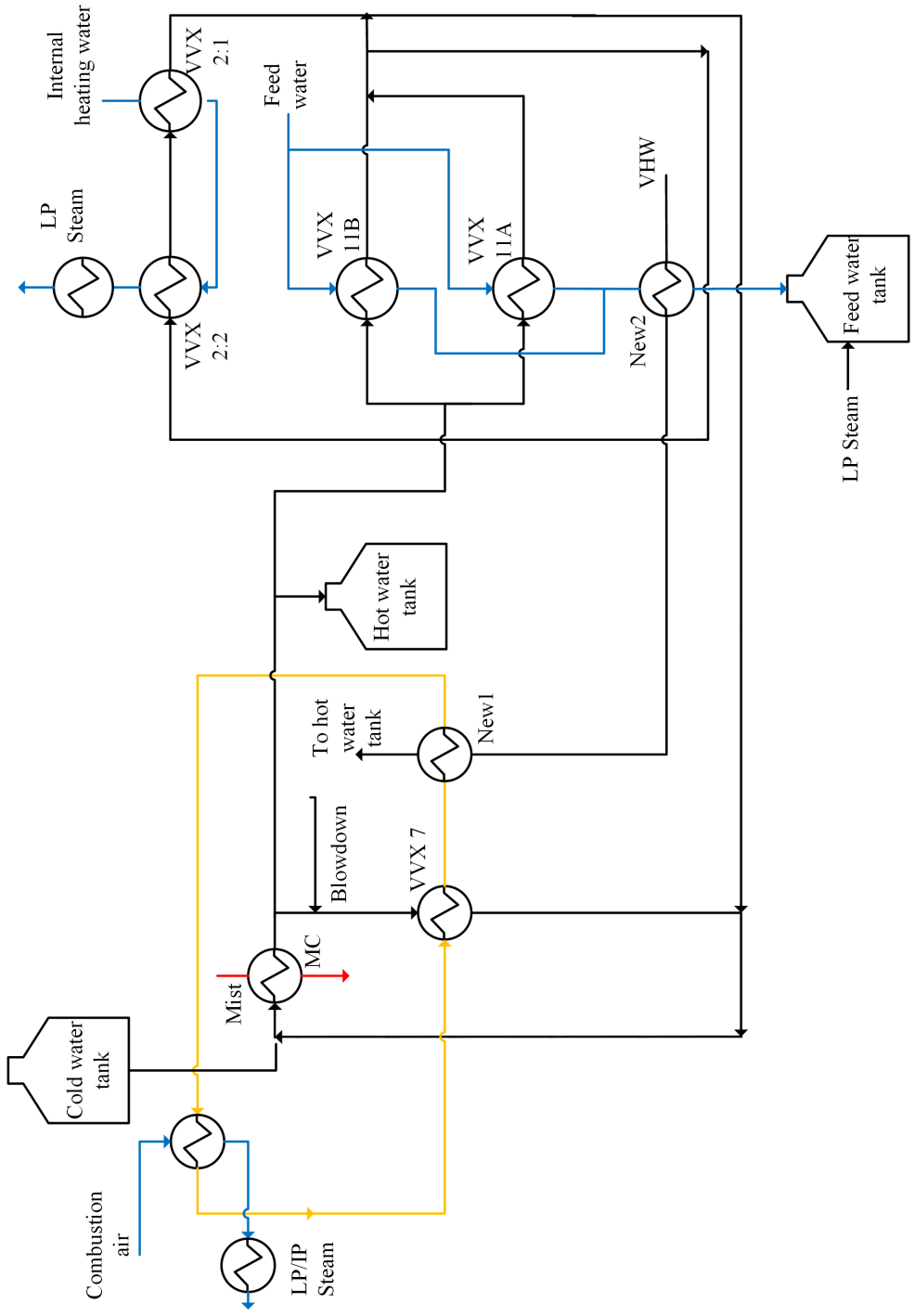

Figure C.2: Design 2

Design 3:

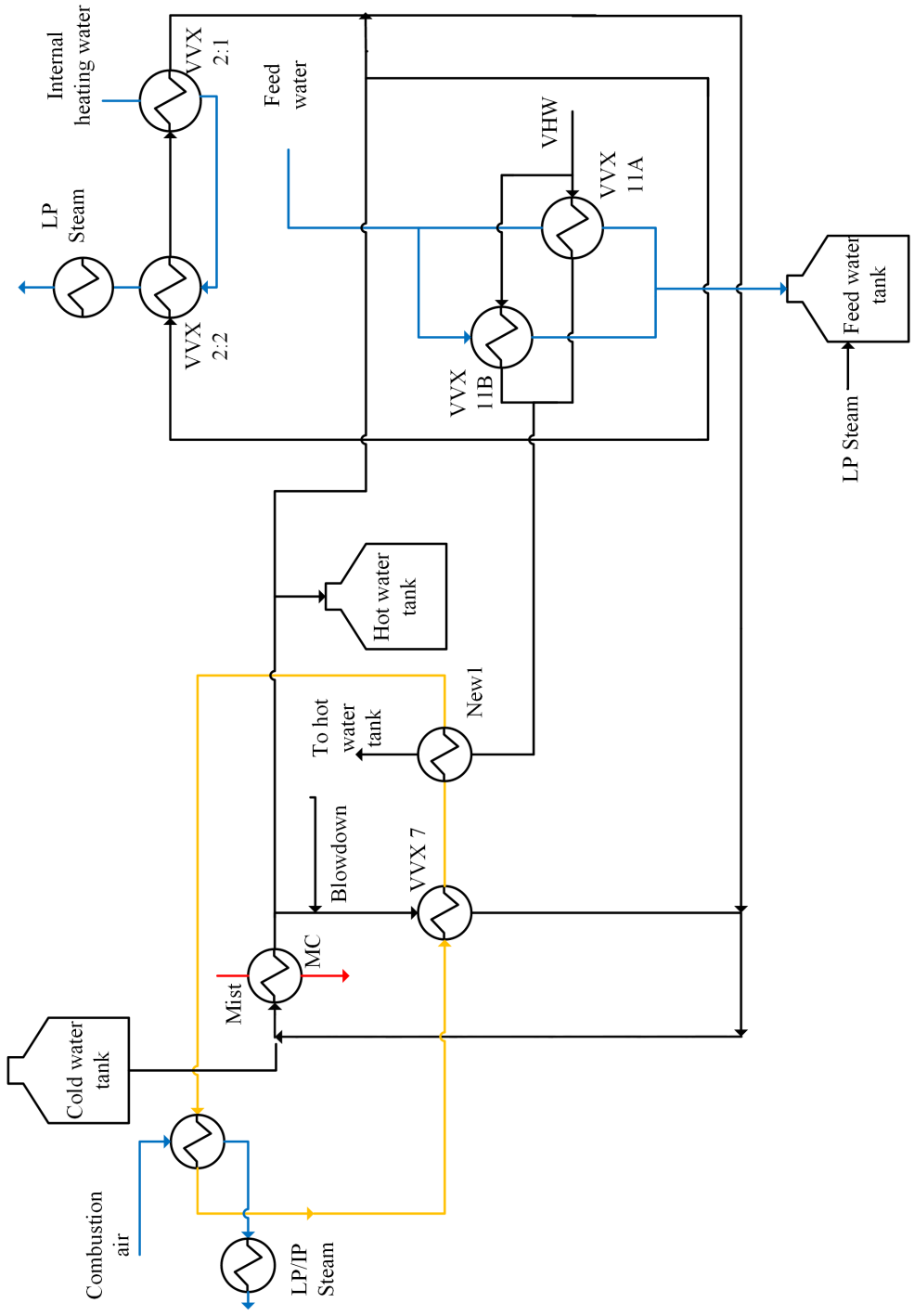

Figure C.3: Design 3

Design 4:

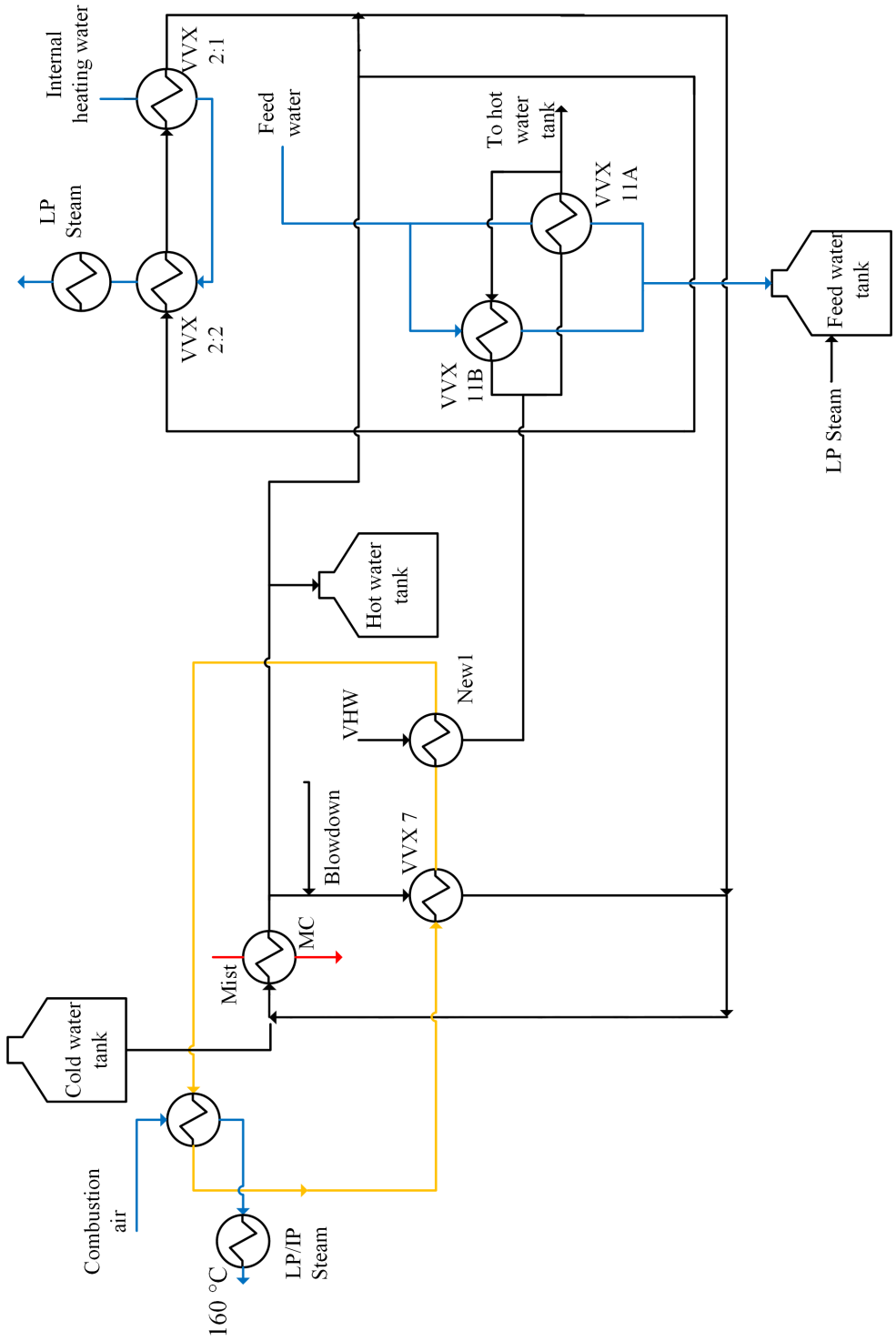

Figure C.4: Design 4